



US 20110042607A1

(19) **United States**

(12) **Patent Application Publication**  
**KANATZIDIS et al.**

(10) **Pub. No.: US 2011/0042607 A1**

(43) **Pub. Date: Feb. 24, 2011**

(54) **THERMOELECTRIC COMPOSITIONS AND PROCESS**

(22) Filed: **Nov. 2, 2010**

**Related U.S. Application Data**

(75) Inventors: **MERCOURI G. KANATZIDIS**,  
Wilmette, IL (US); **JOHN ANDROULAKIS**,  
Evanston, IL (US); **JOSEPH R. SOOTSMAN**,  
Pasadena, CA (US)

(62) Division of application No. 11/445,662, filed on Jun. 2, 2006, now Pat. No. 7,847,179.

(60) Provisional application No. 60/687,769, filed on Jun. 6, 2005.

**Publication Classification**

Correspondence Address:

**KNOBBE MARTENS OLSON & BEAR LLP**  
**2040 MAIN STREET, FOURTEENTH FLOOR**  
**IRVINE, CA 92614 (US)**

(51) **Int. Cl.**  
**H01L 35/16** (2006.01)

(52) **U.S. Cl.** ..... **252/62.3 T**

(73) Assignee: **BOARD OF TRUSTEES OF MICHIGAN STATE UNIVERSITY**, East Lansing, MI (US)

(57) **ABSTRACT**

A process for producing bulk thermoelectric compositions containing nanoscale inclusions is described. The thermoelectric compositions have a higher figure of merit (ZT) than without the inclusions. The compositions are useful for power generation and in heat pumps for instance.

(21) Appl. No.: **12/938,250**

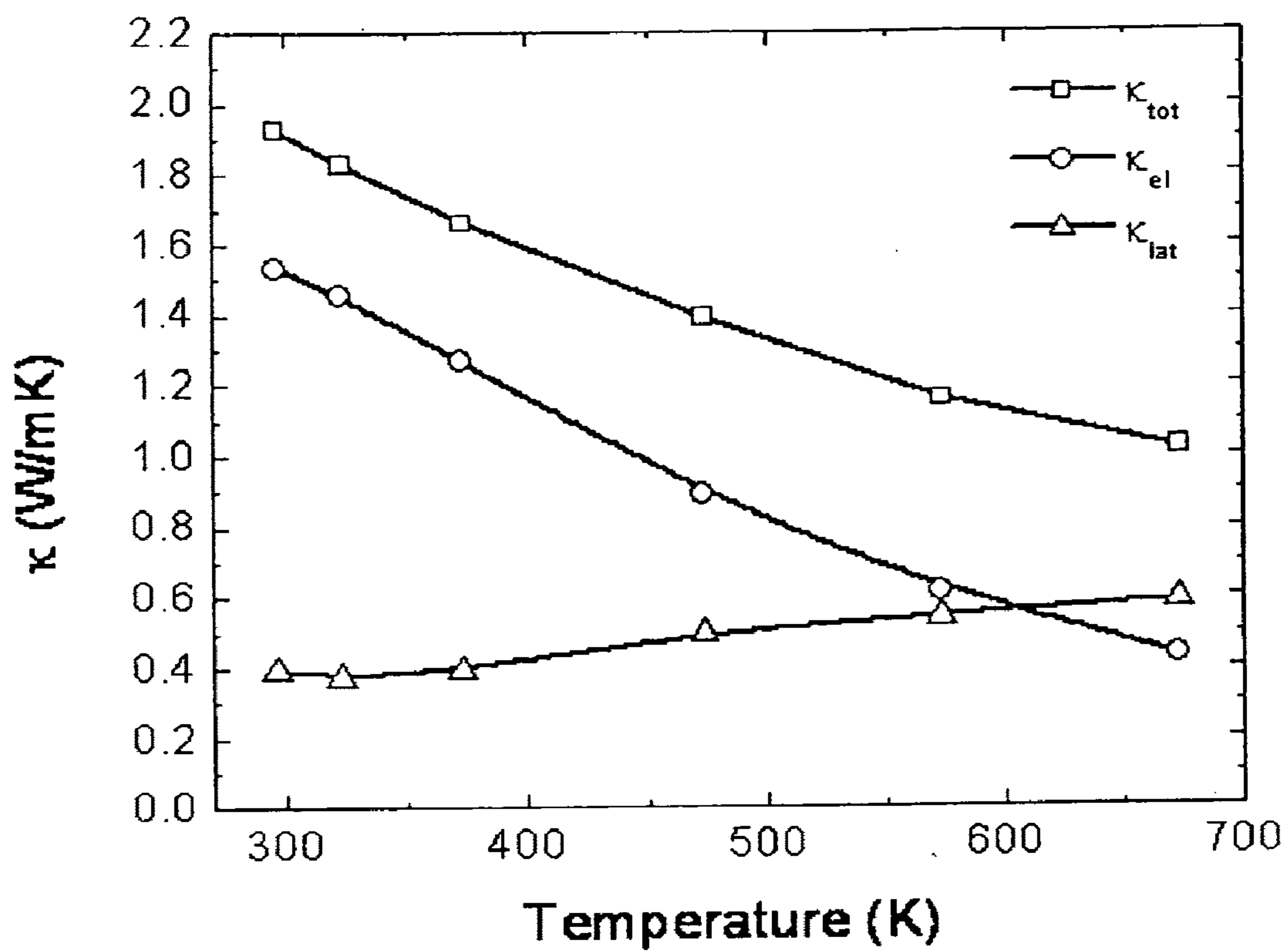


FIGURE 1

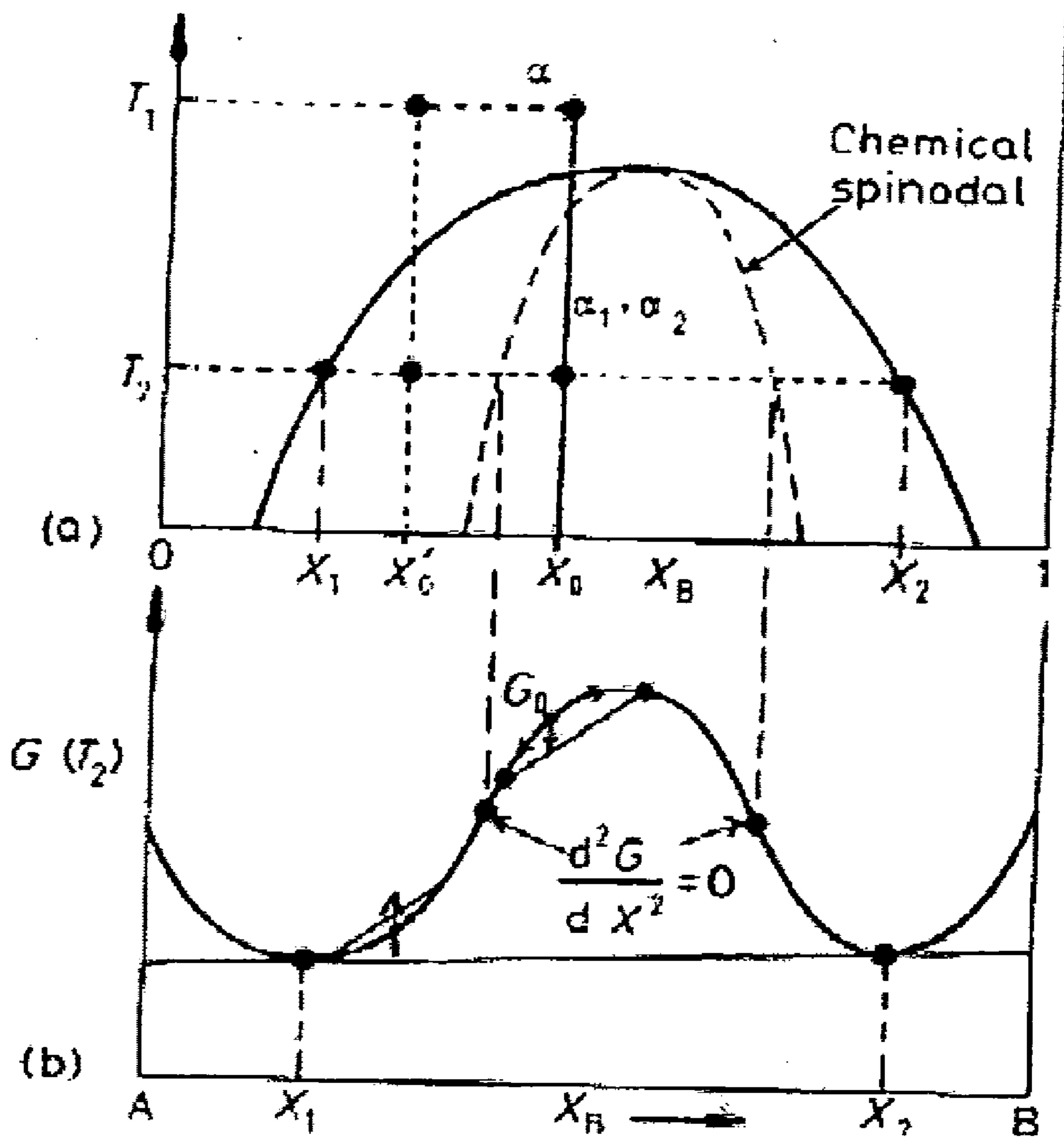


FIGURE 2A

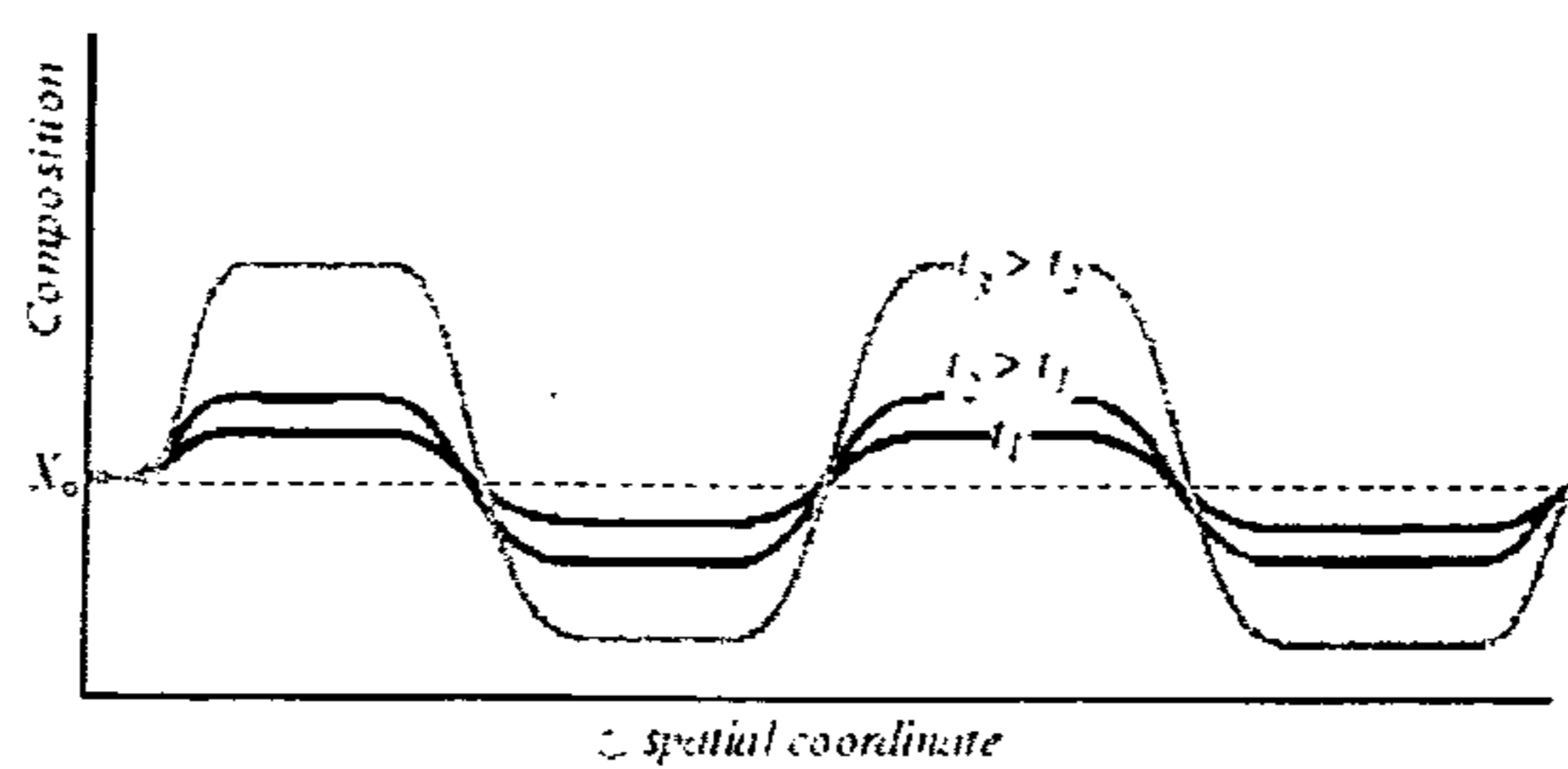


Figure 2B

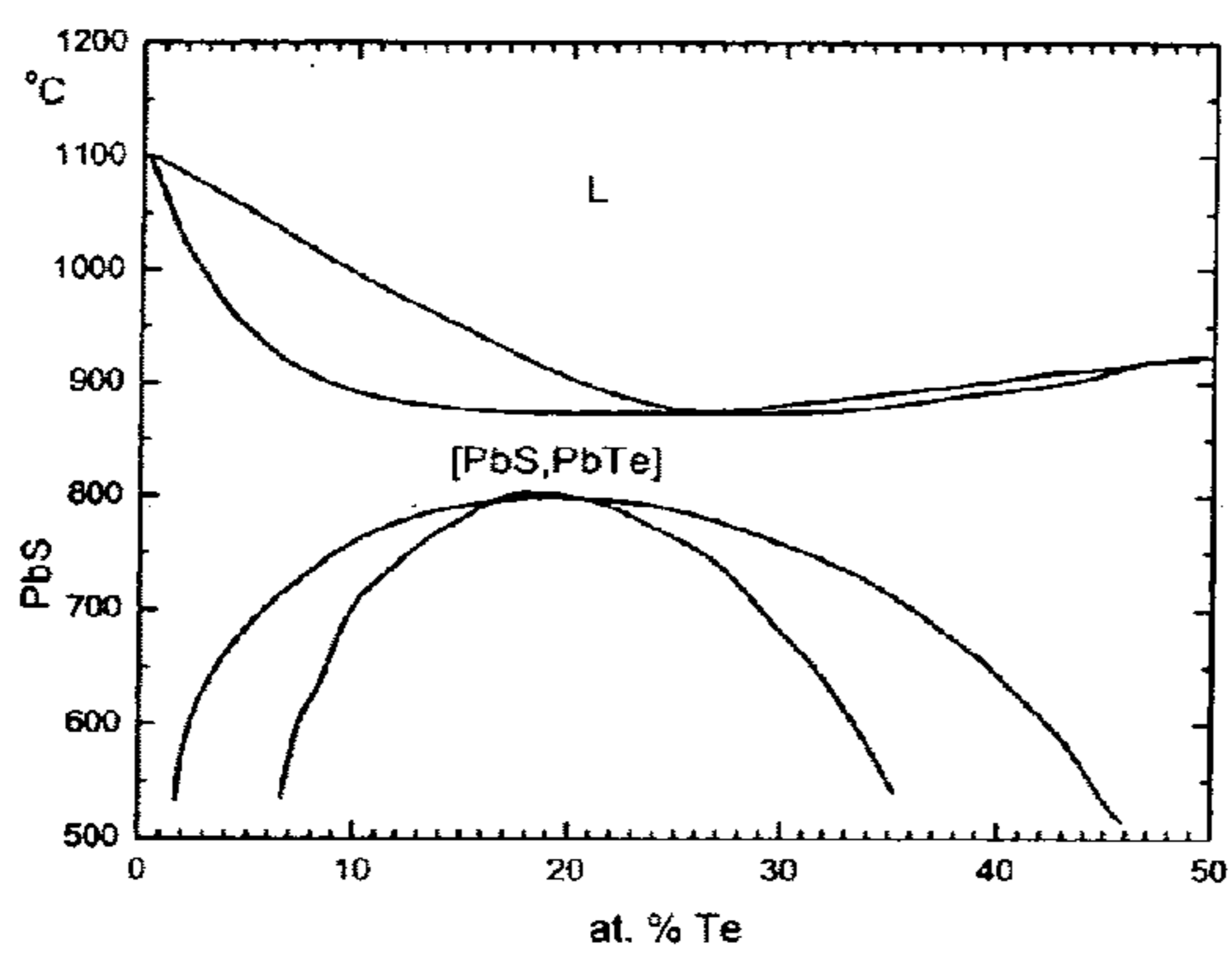


FIGURE 3A

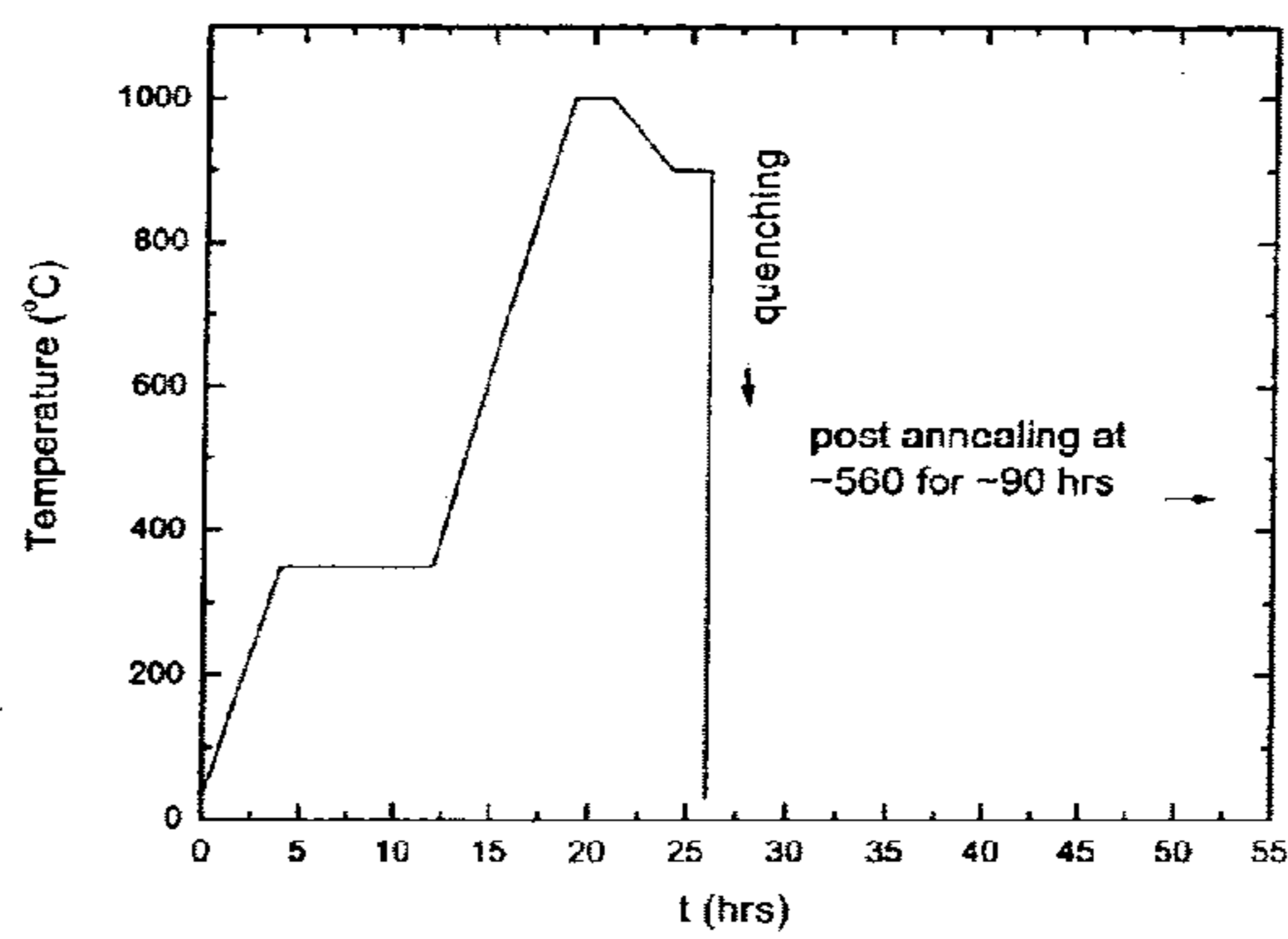


FIGURE 3B

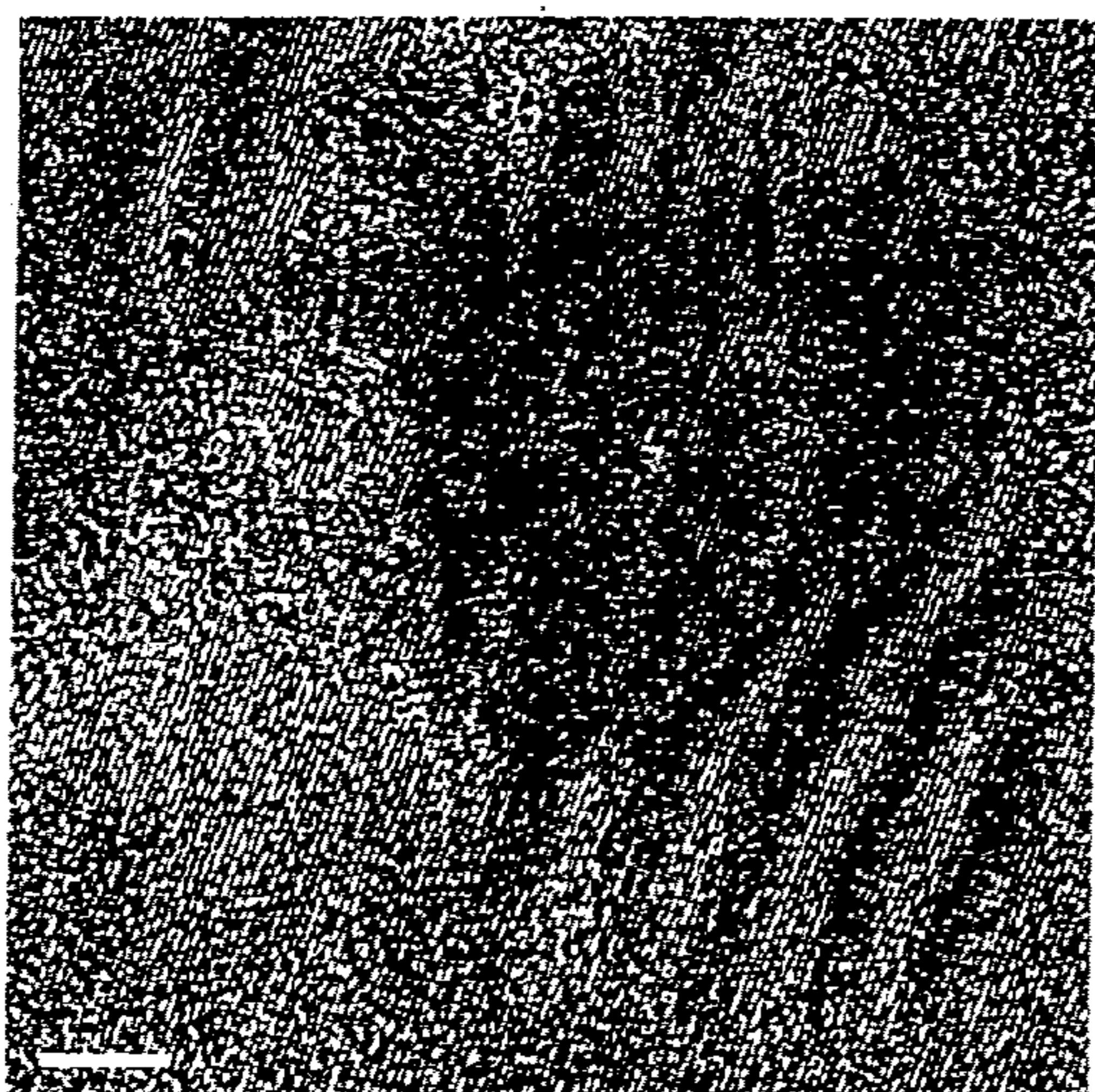


FIGURE 3C

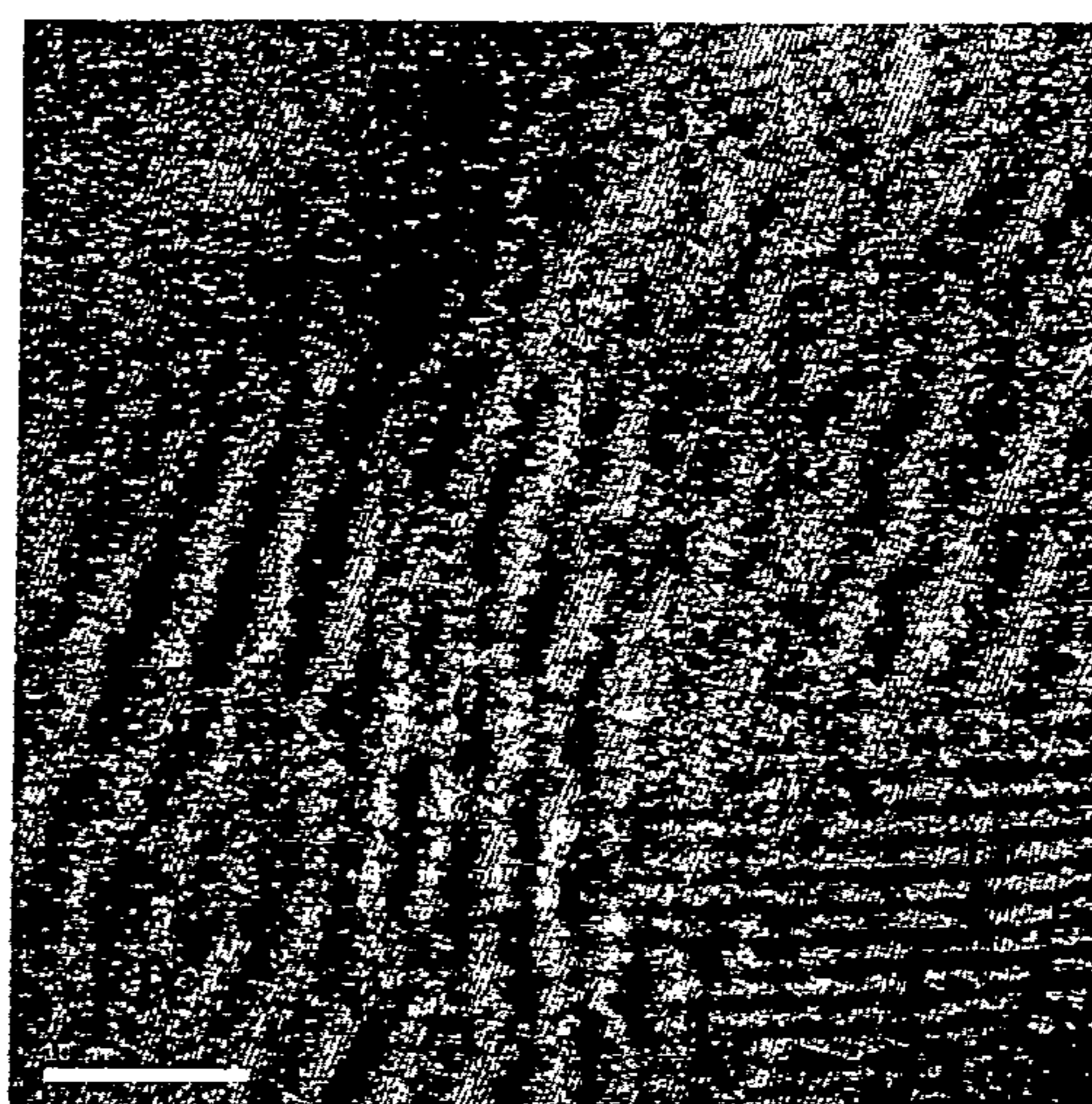


FIGURE 3D

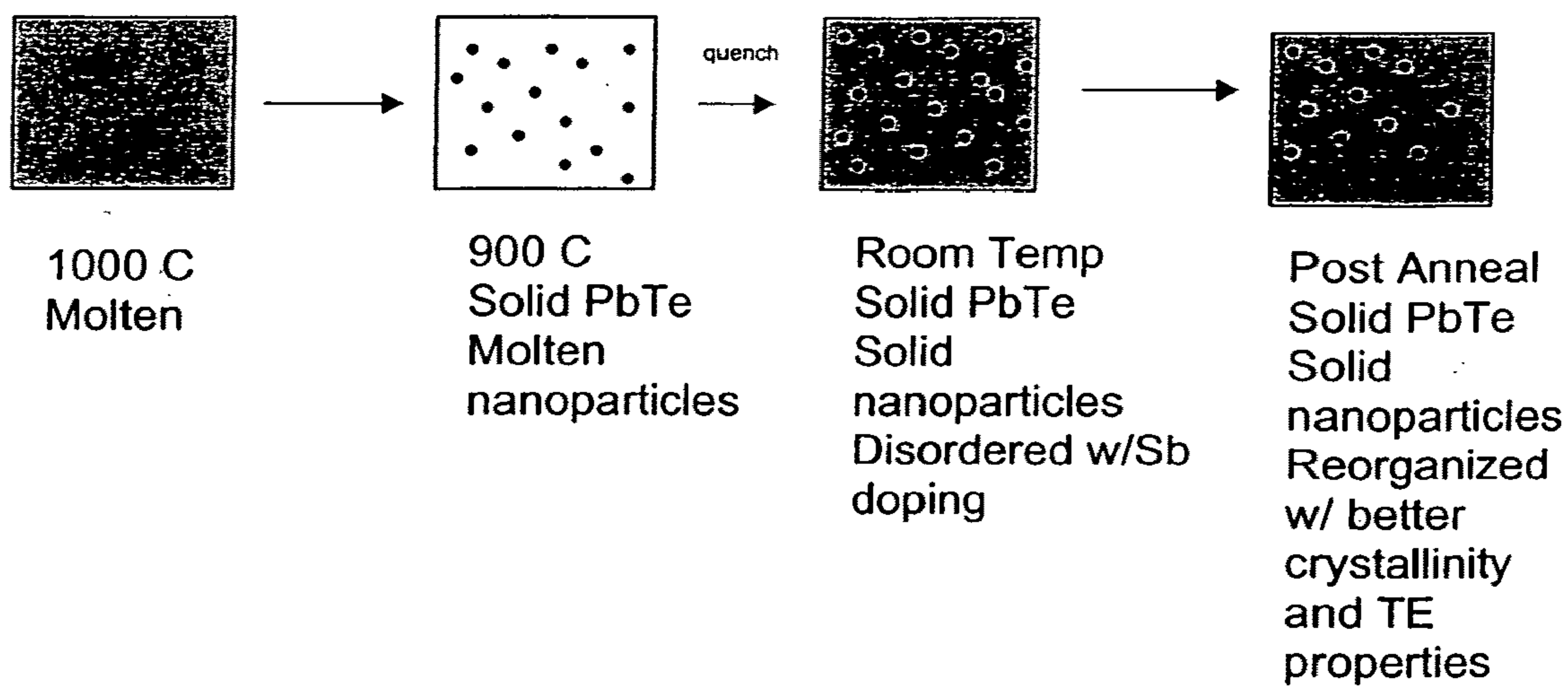


FIGURE 4A

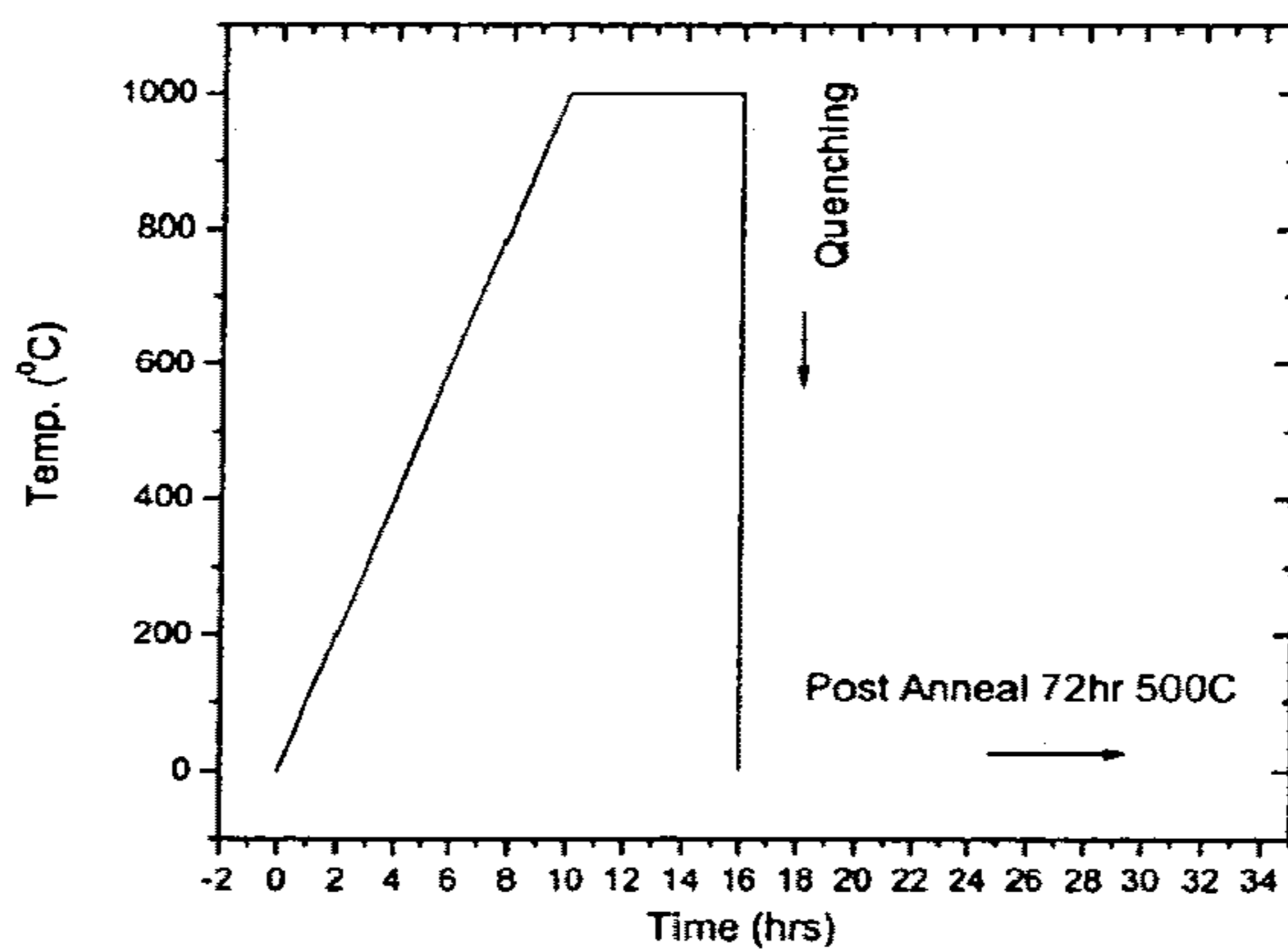
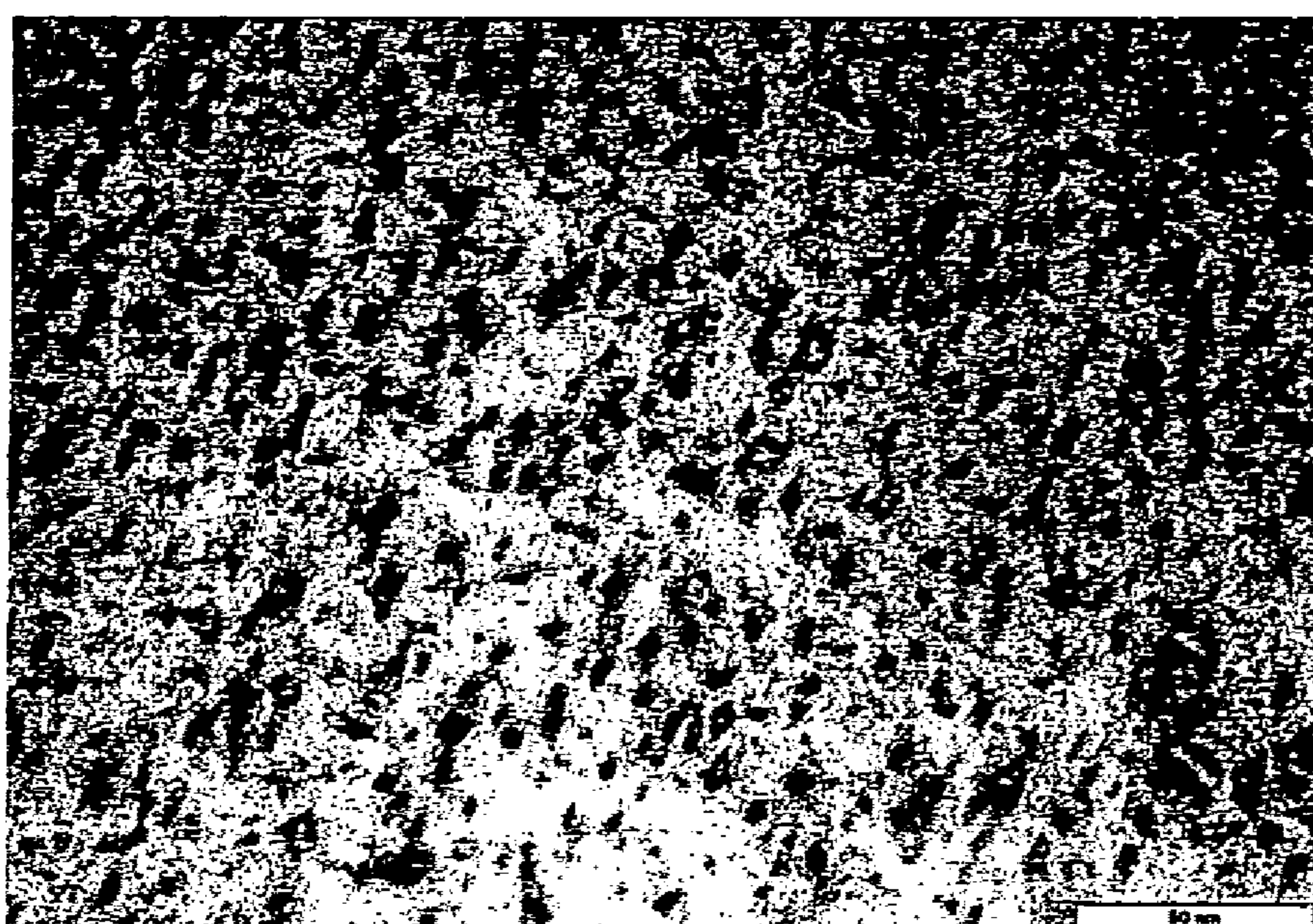


FIGURE 4B



PbTe-Sb(2%) Bright Field Image

**FIGURE 4C**



FIGURE 4D

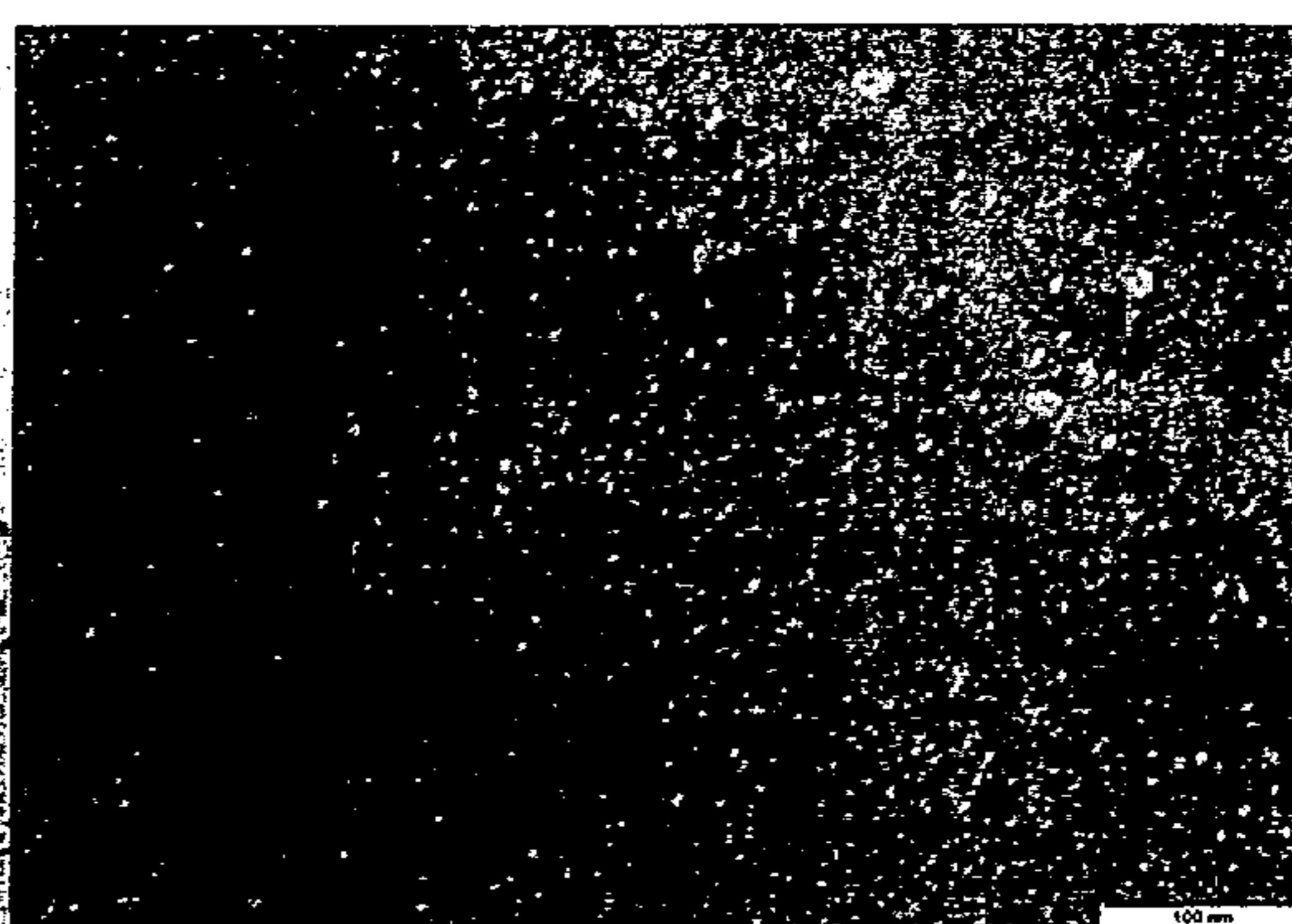
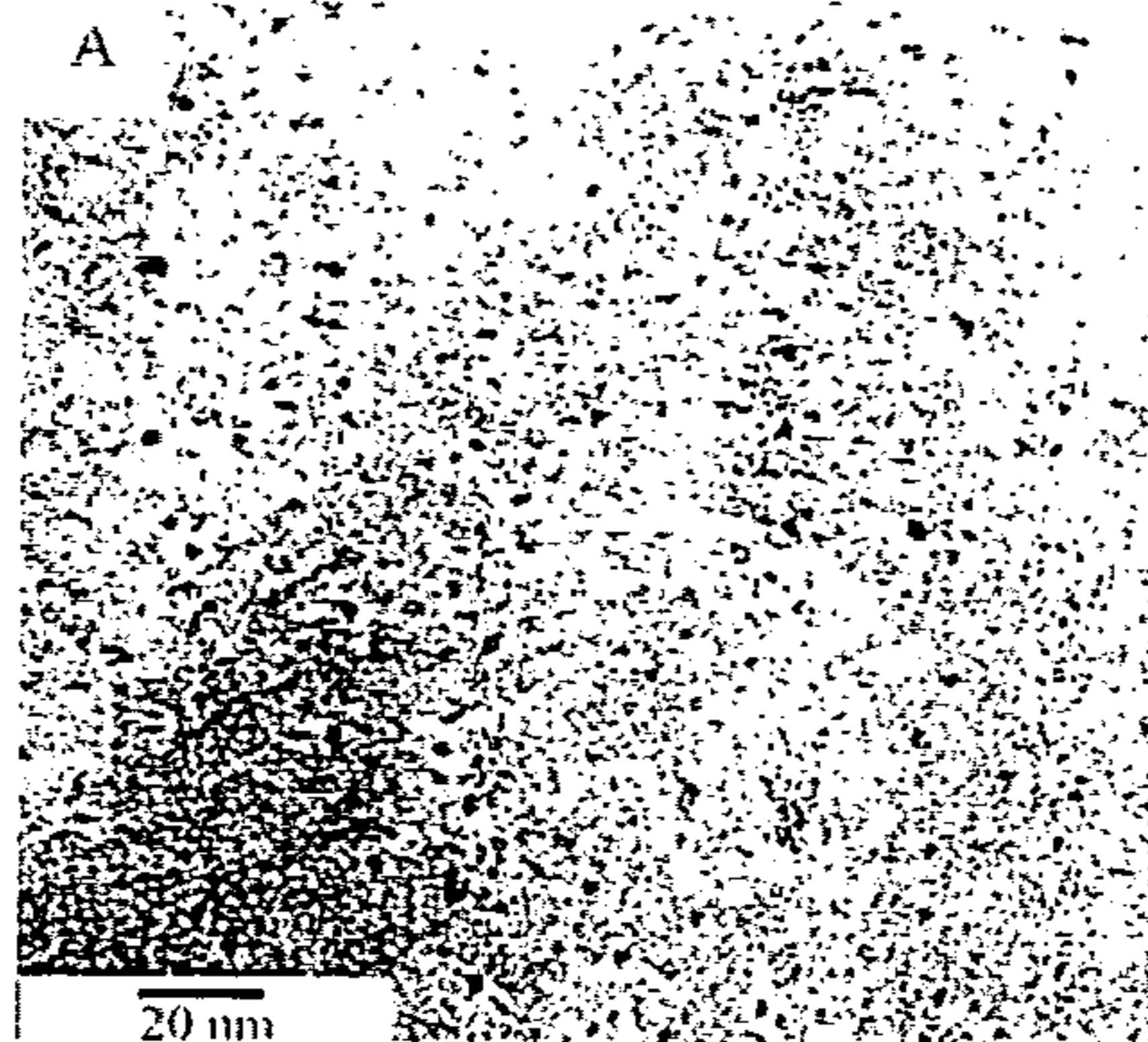


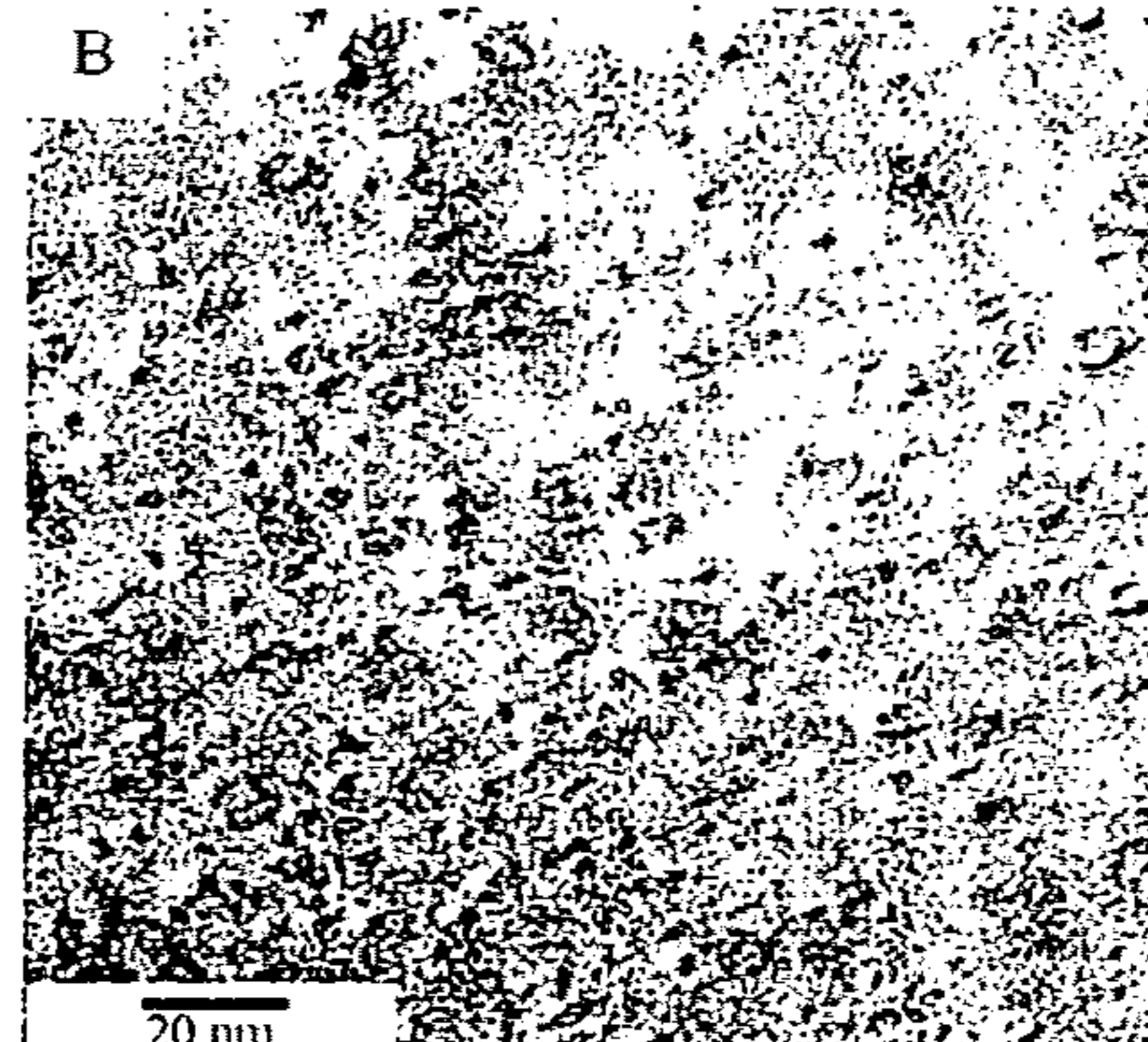
FIGURE 4E



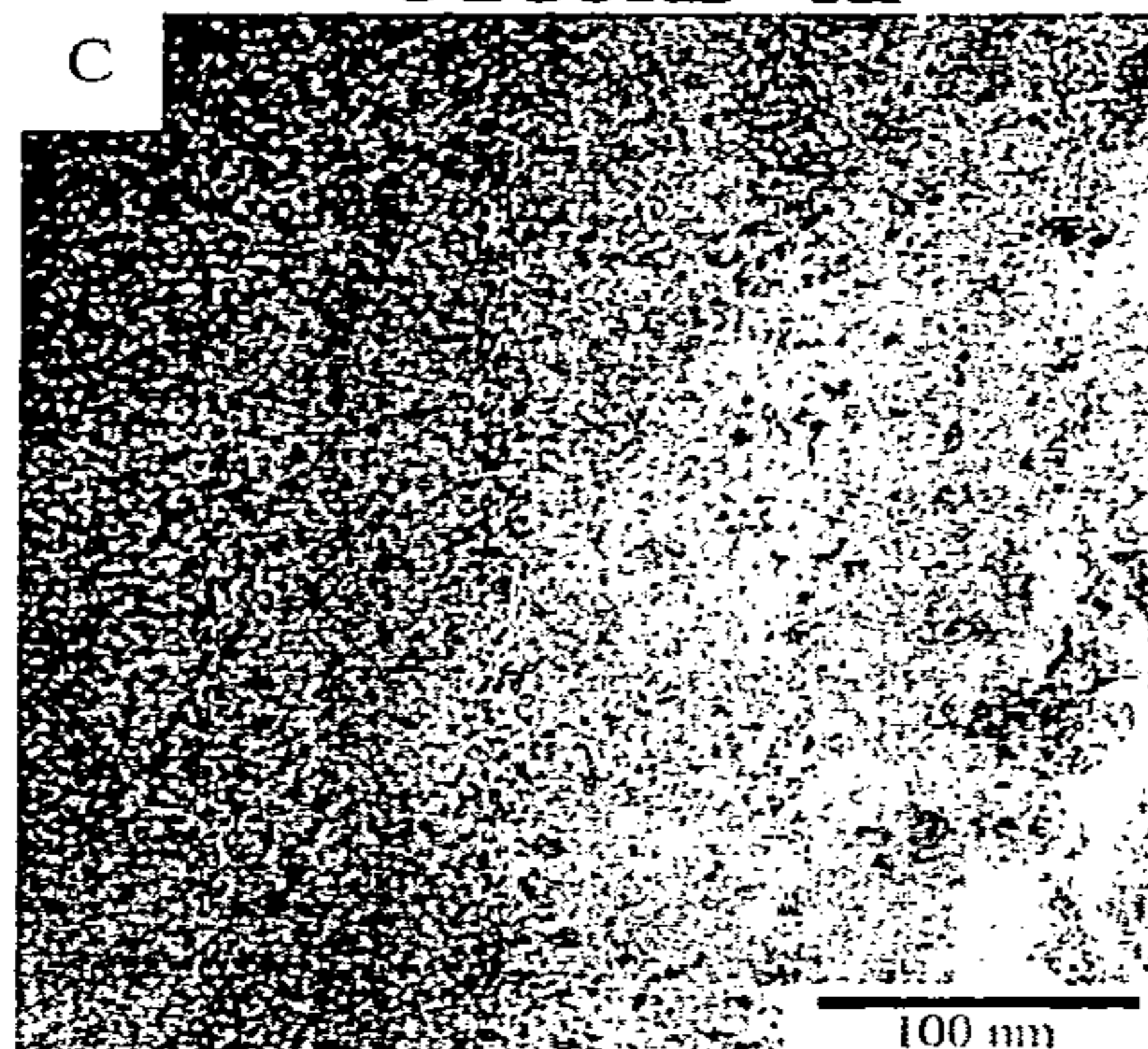
**FIGURE 4F**



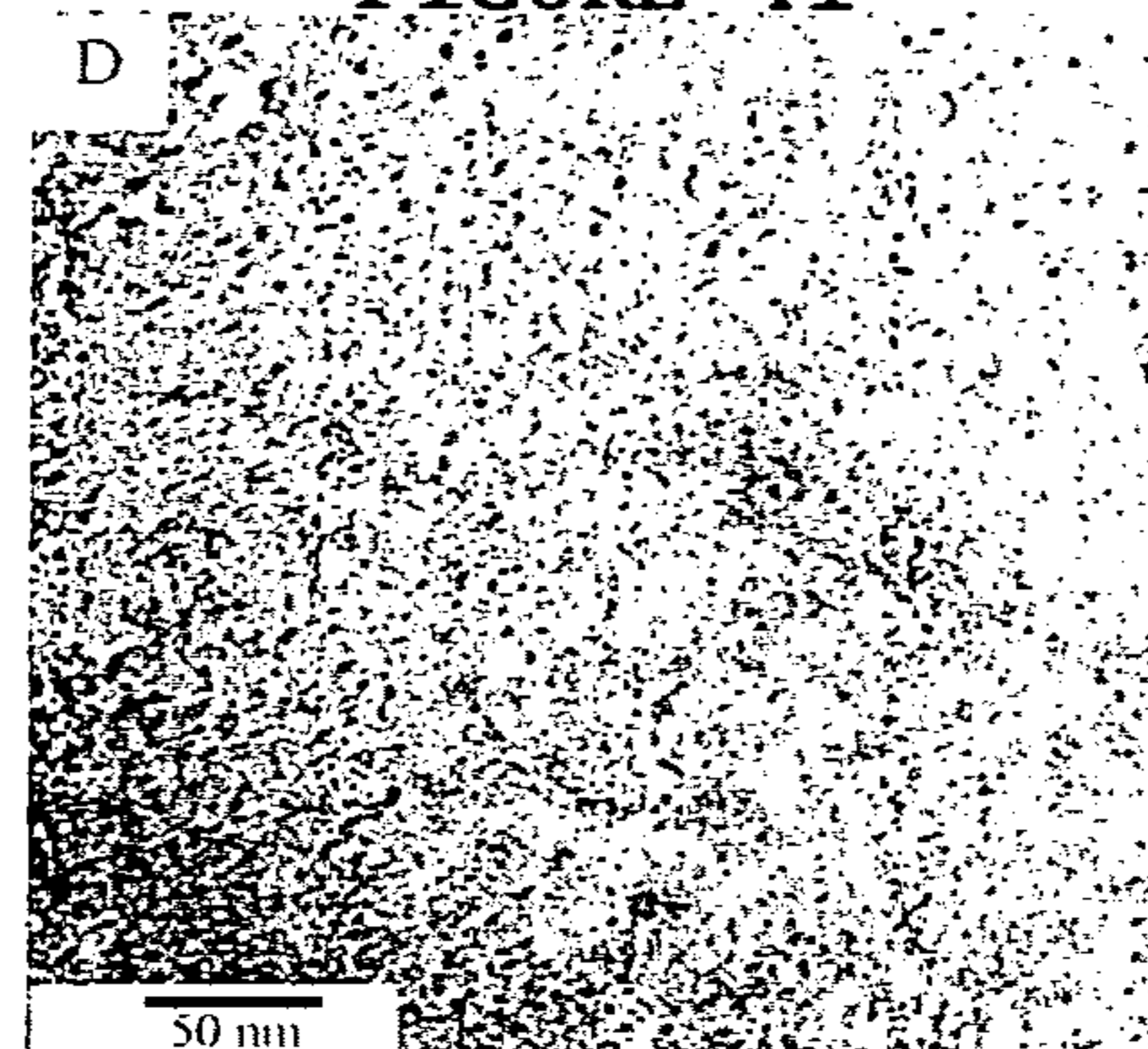
**FIGURE 4G**



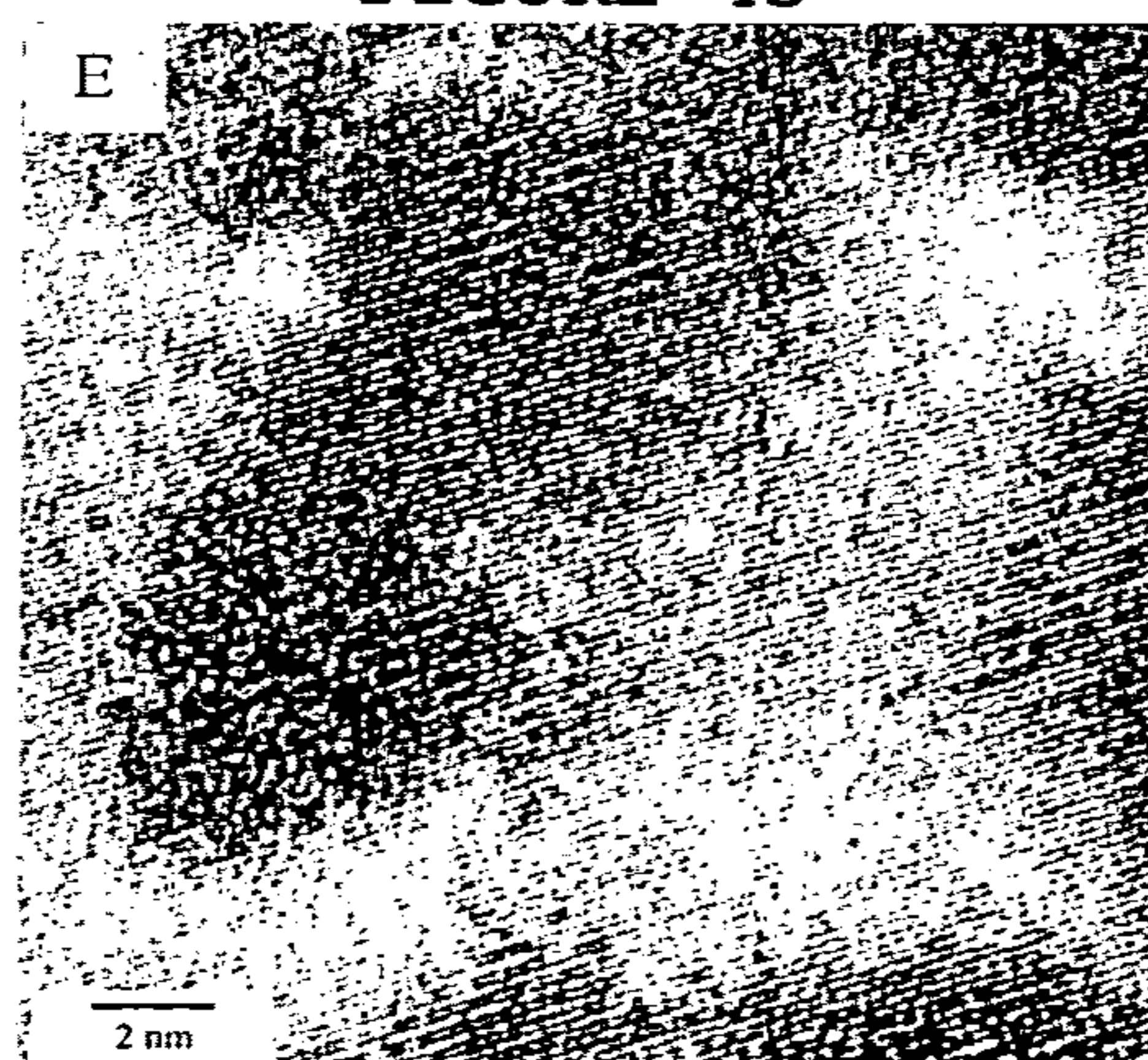
**FIGURE 4H**



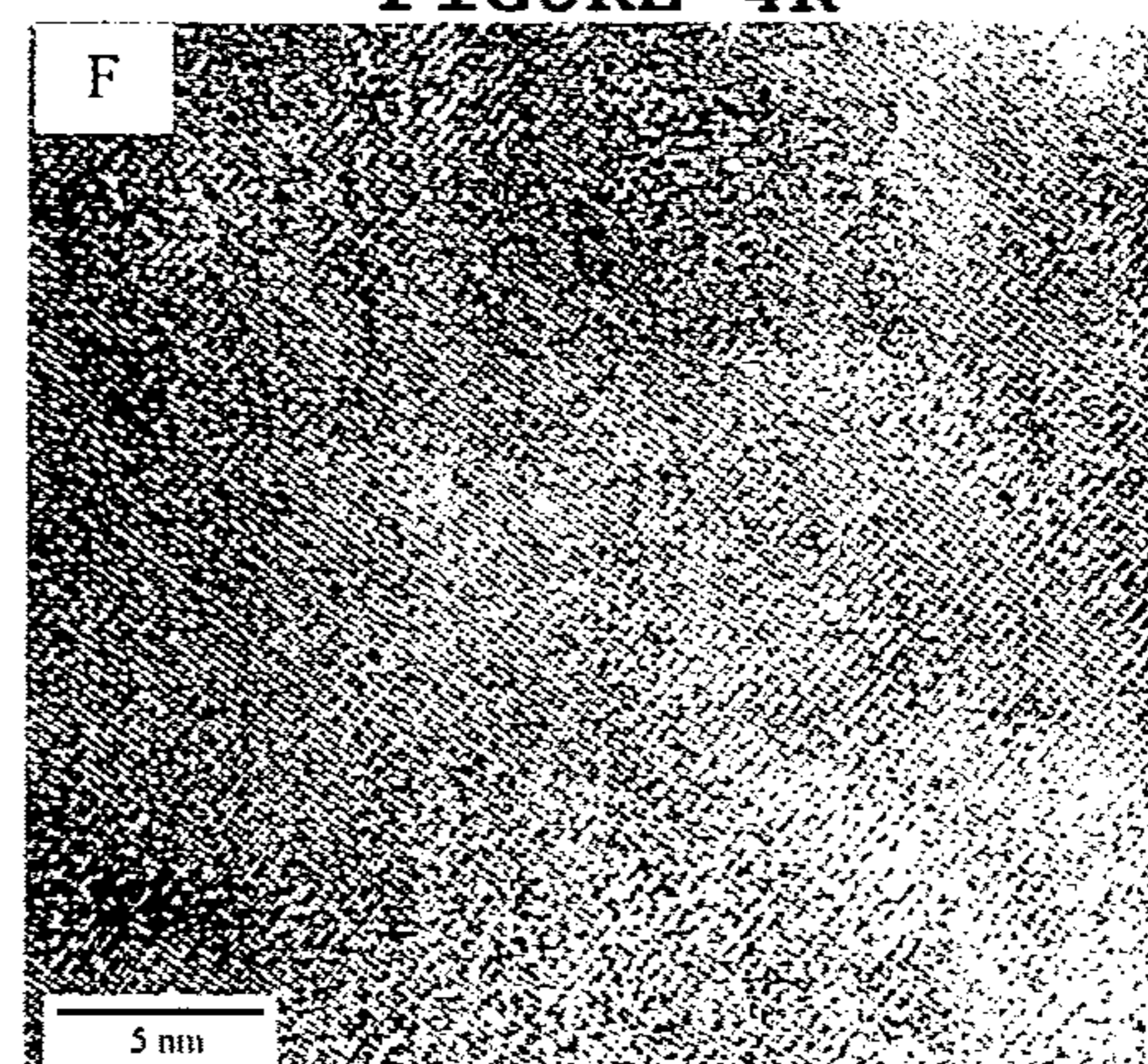
**FIGURE 4I**



**FIGURE 4J**



**FIGURE 4K**



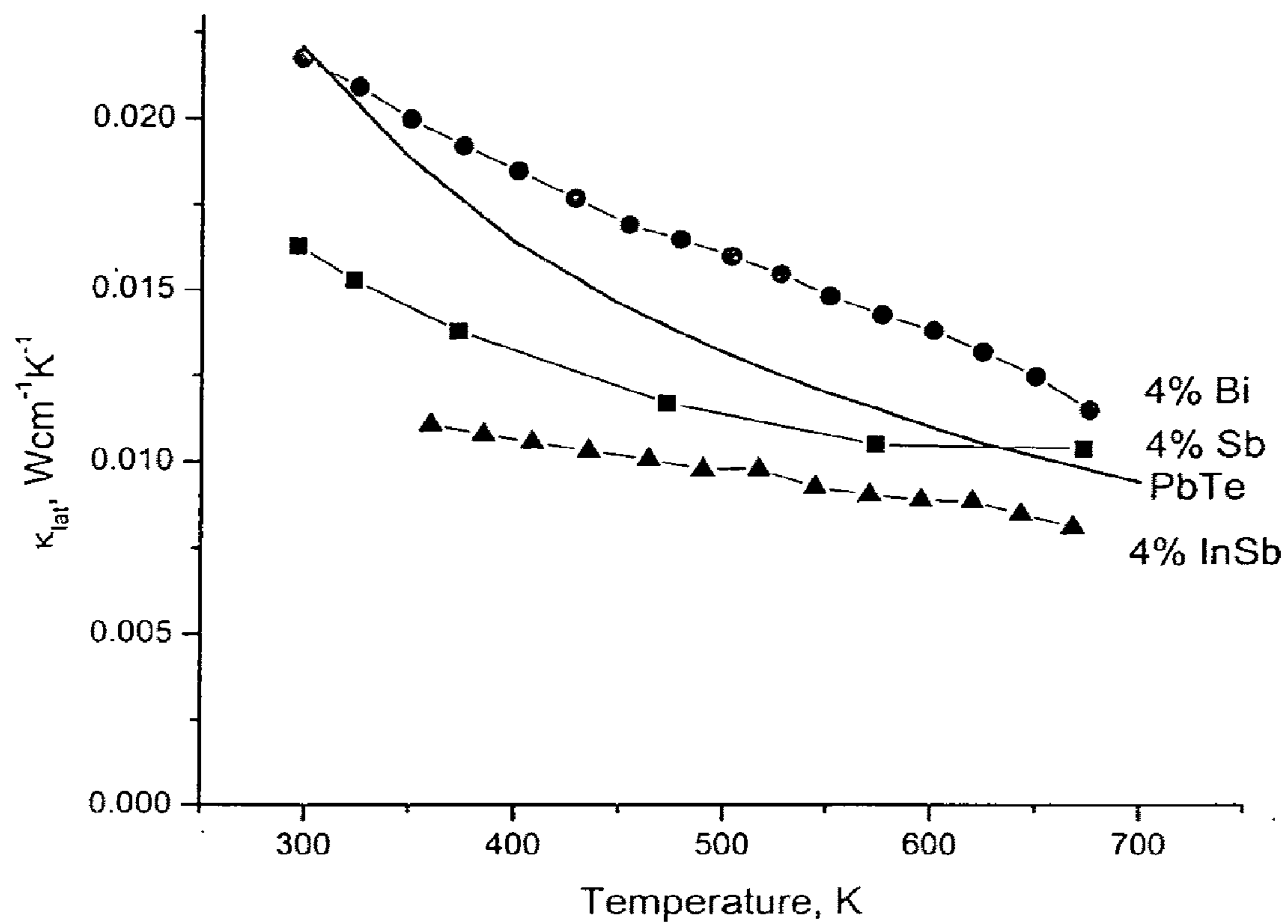


FIGURE 4L

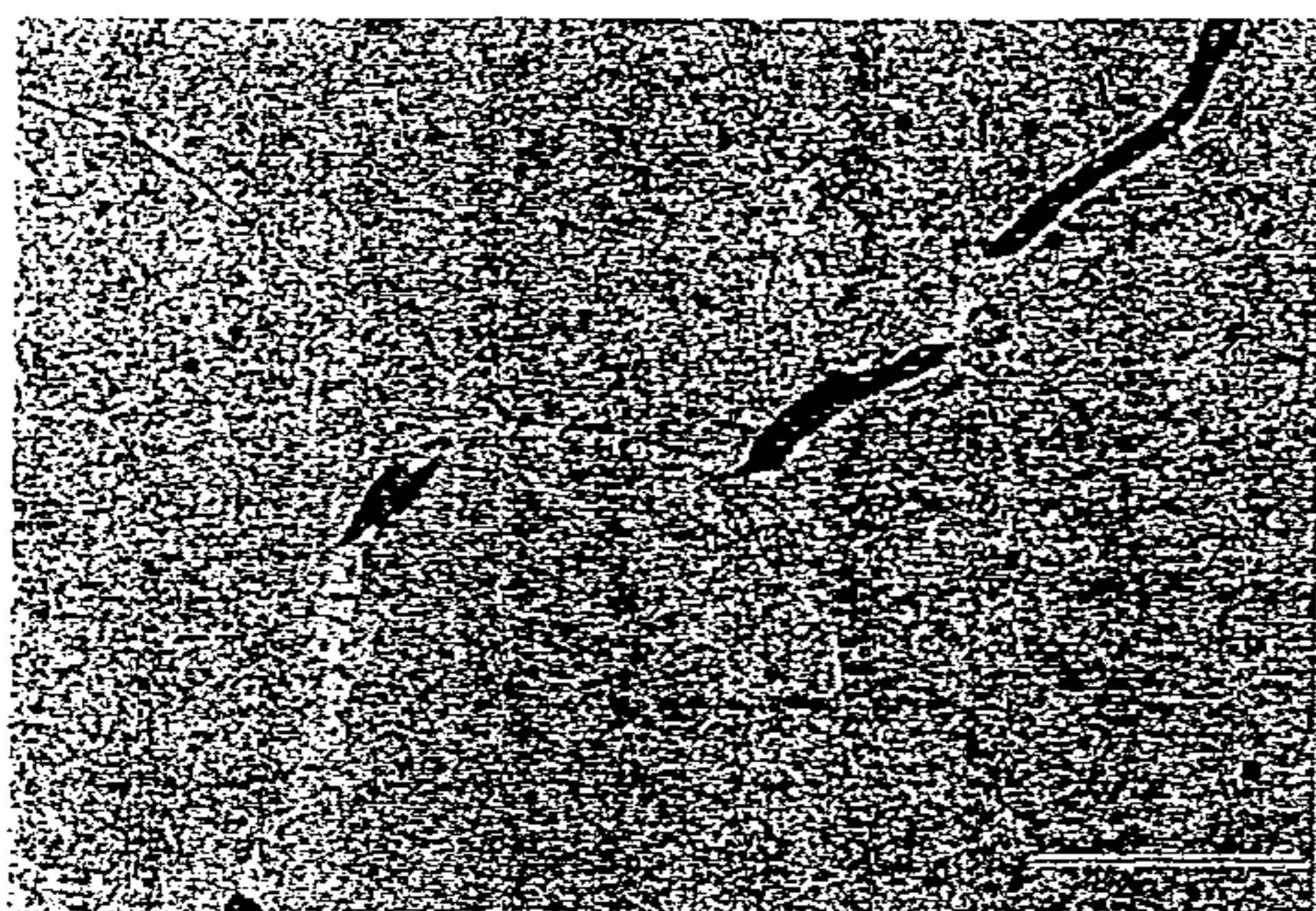


FIGURE 5A

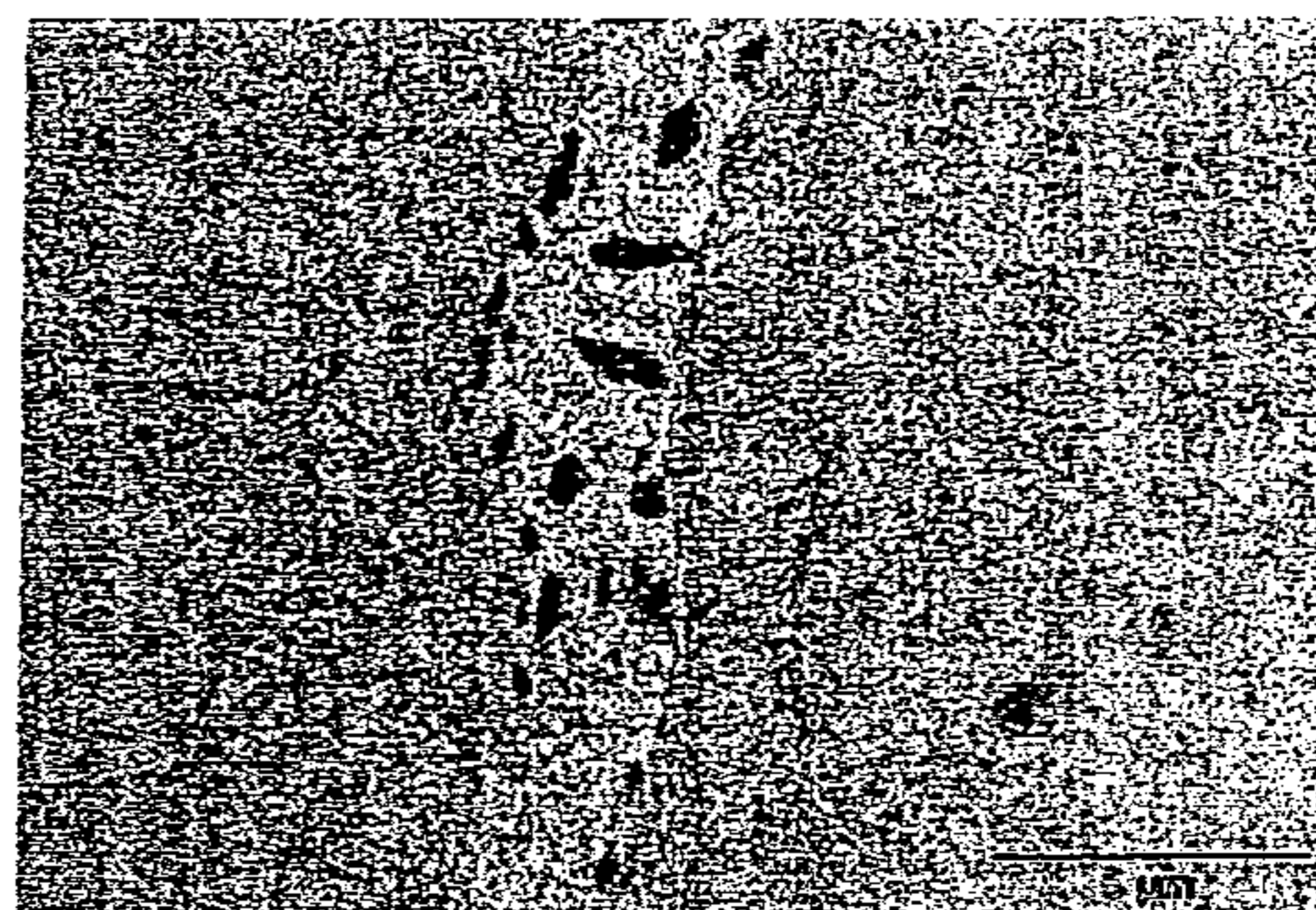


FIGURE 5B

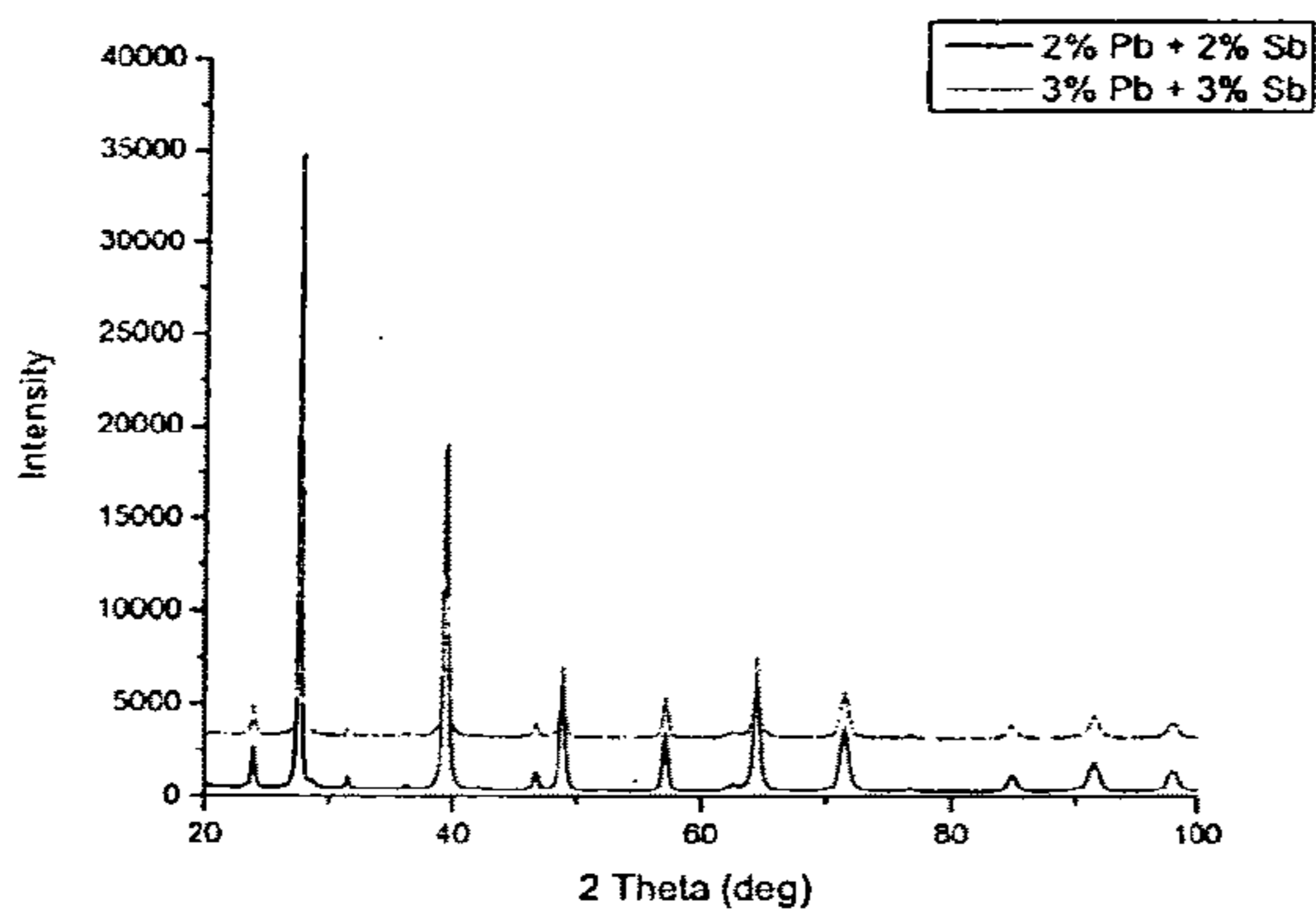


FIGURE 6A

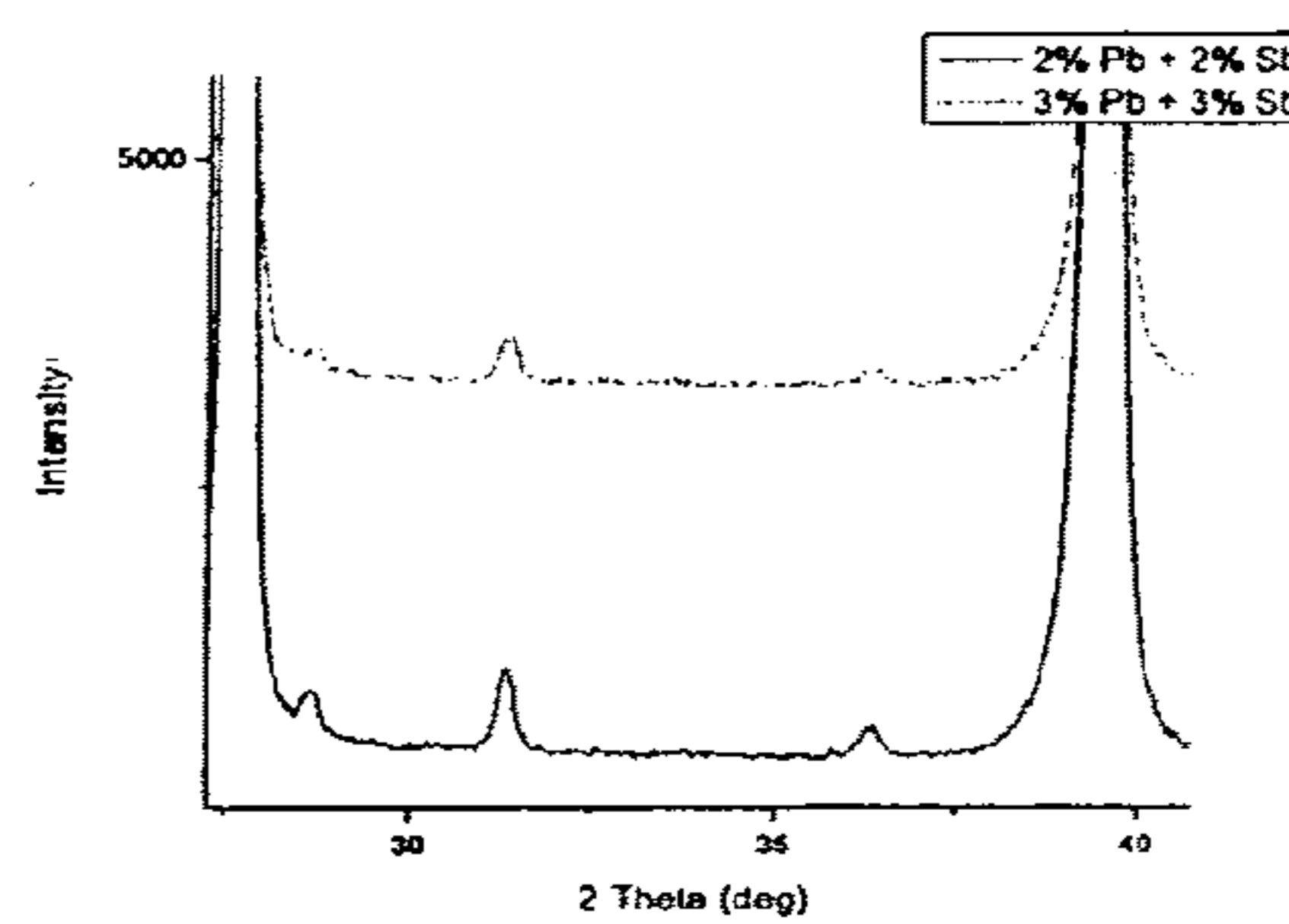


FIGURE 6B

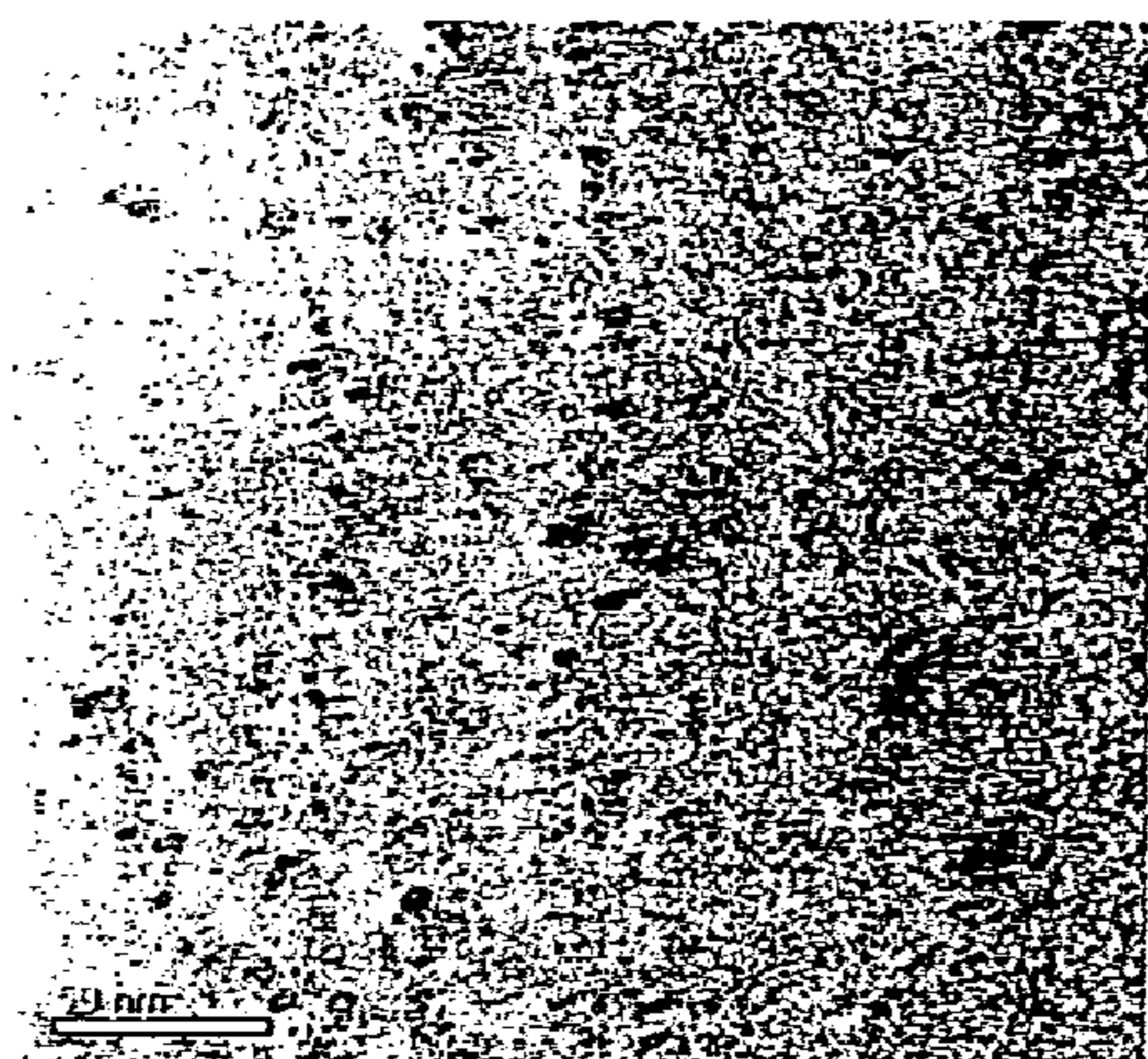


FIGURE 7A

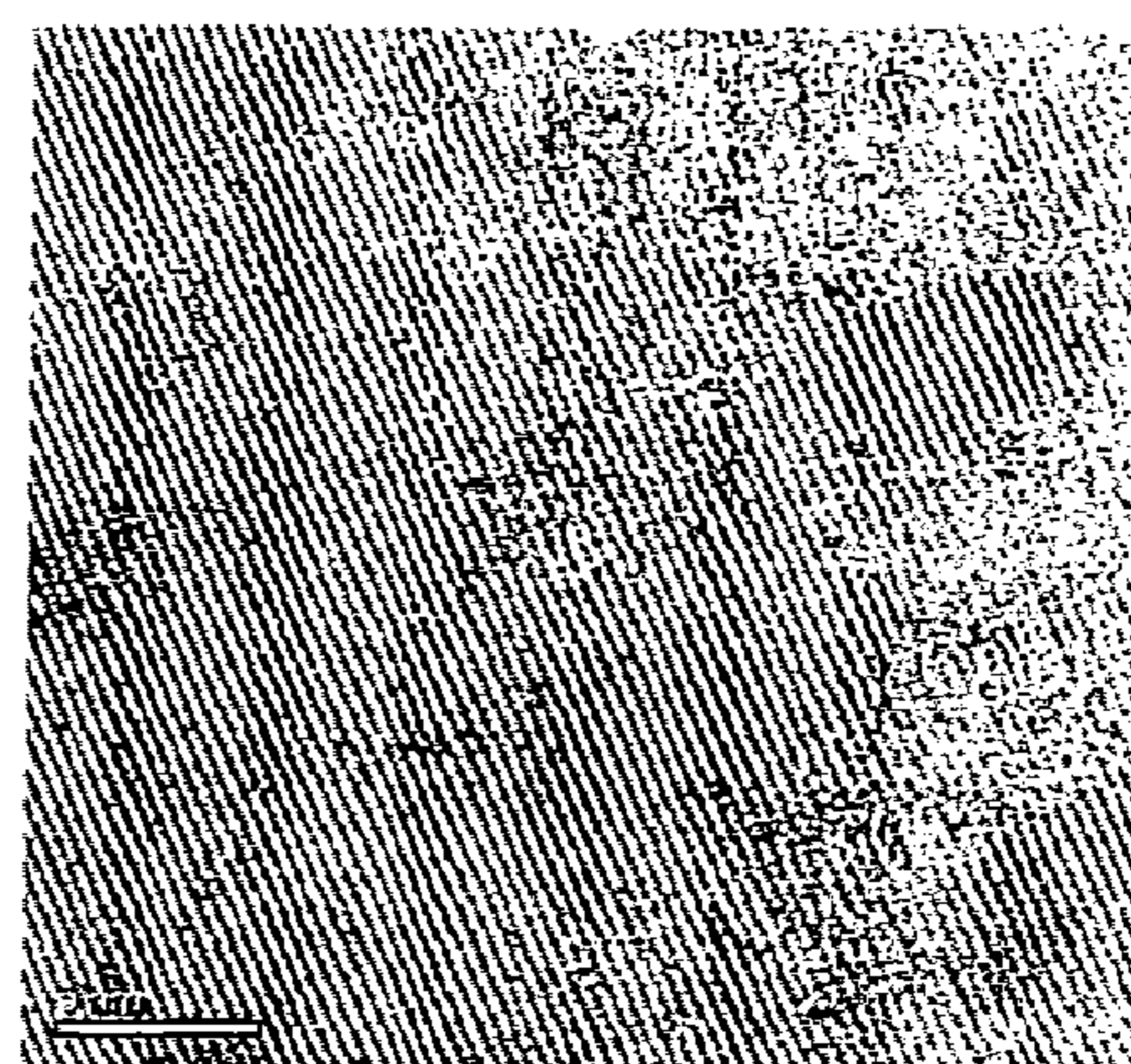


FIGURE 7B

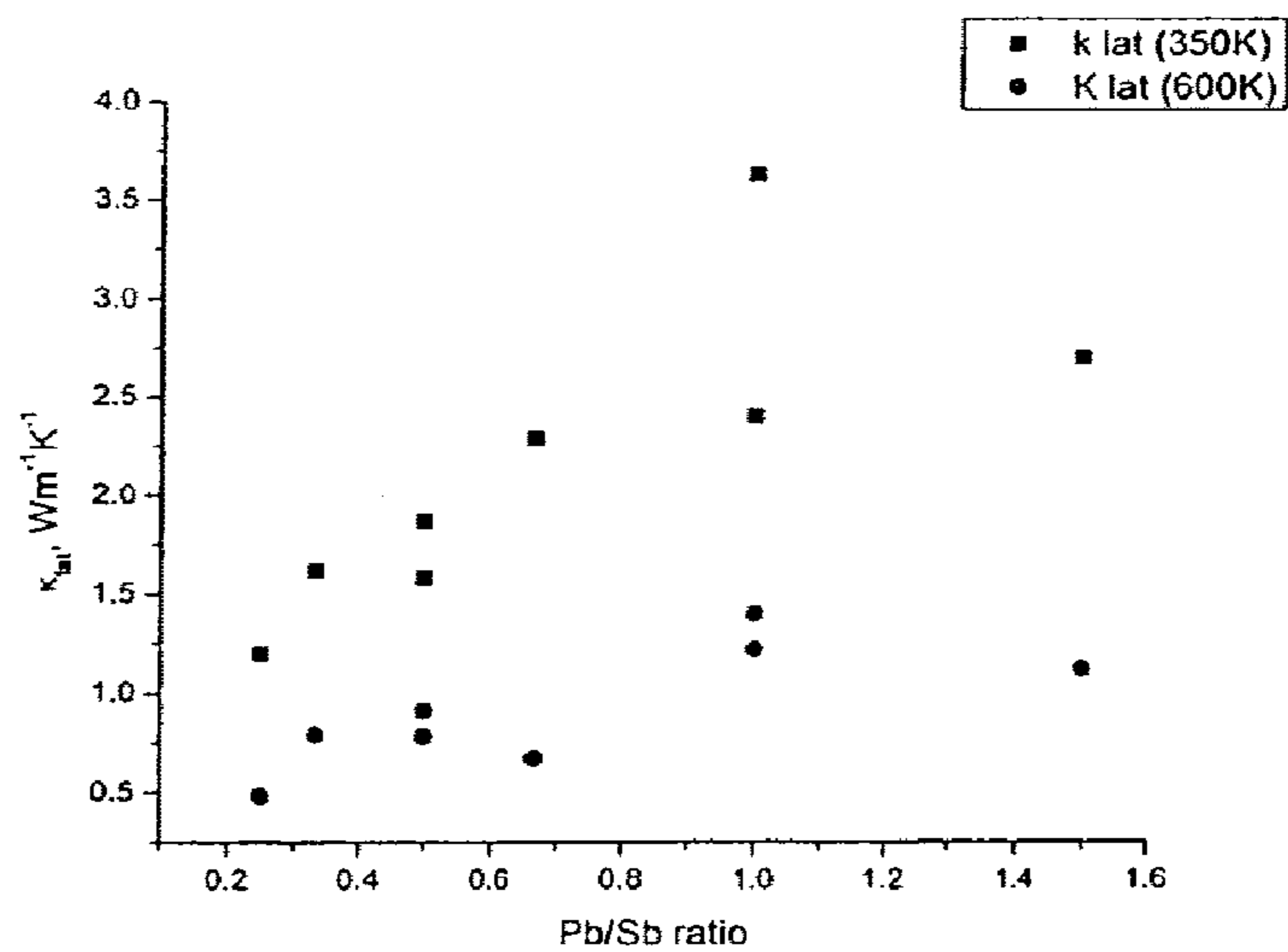


FIGURE 8

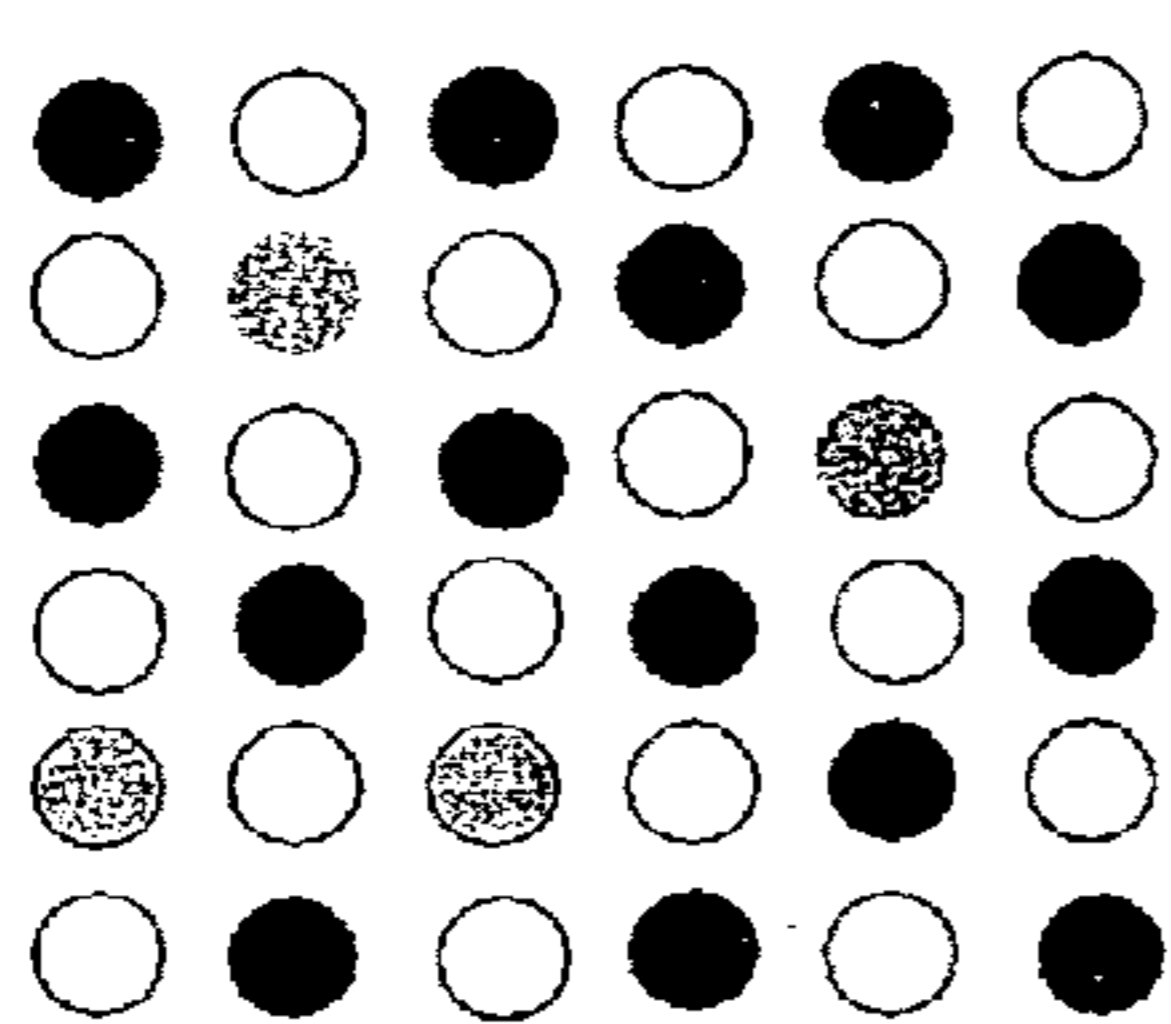


FIGURE 9A

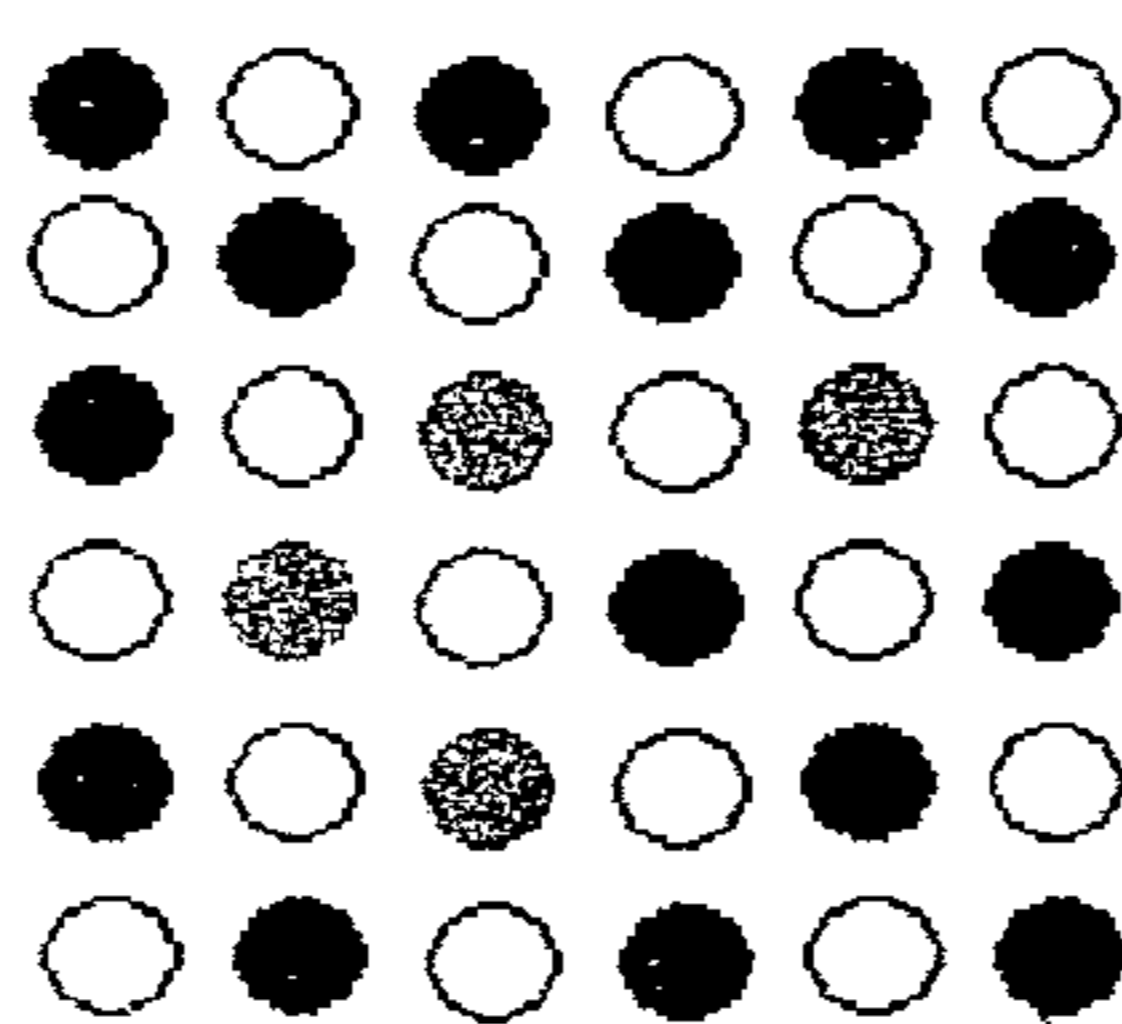


FIGURE 9B

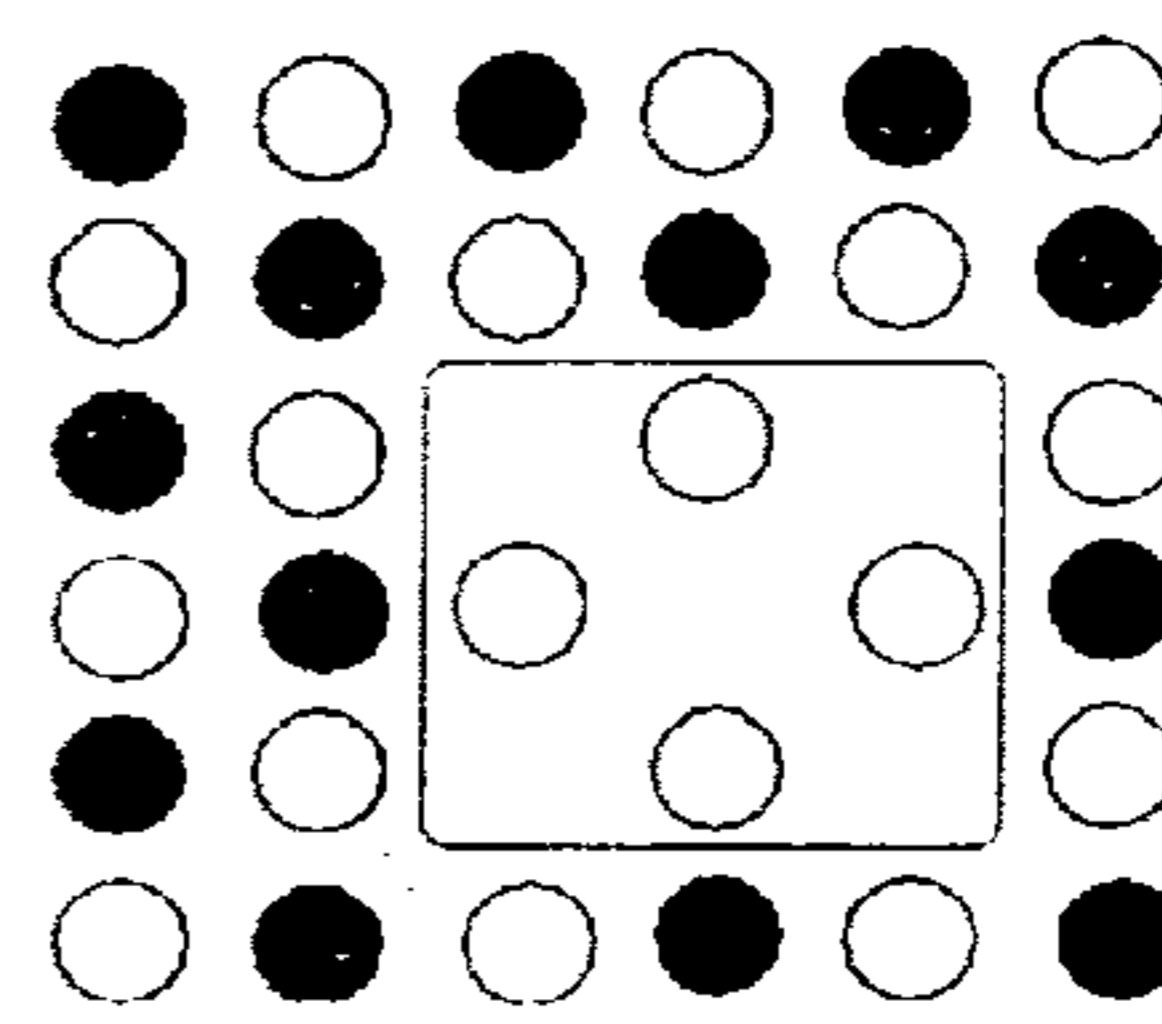


FIGURE 9C

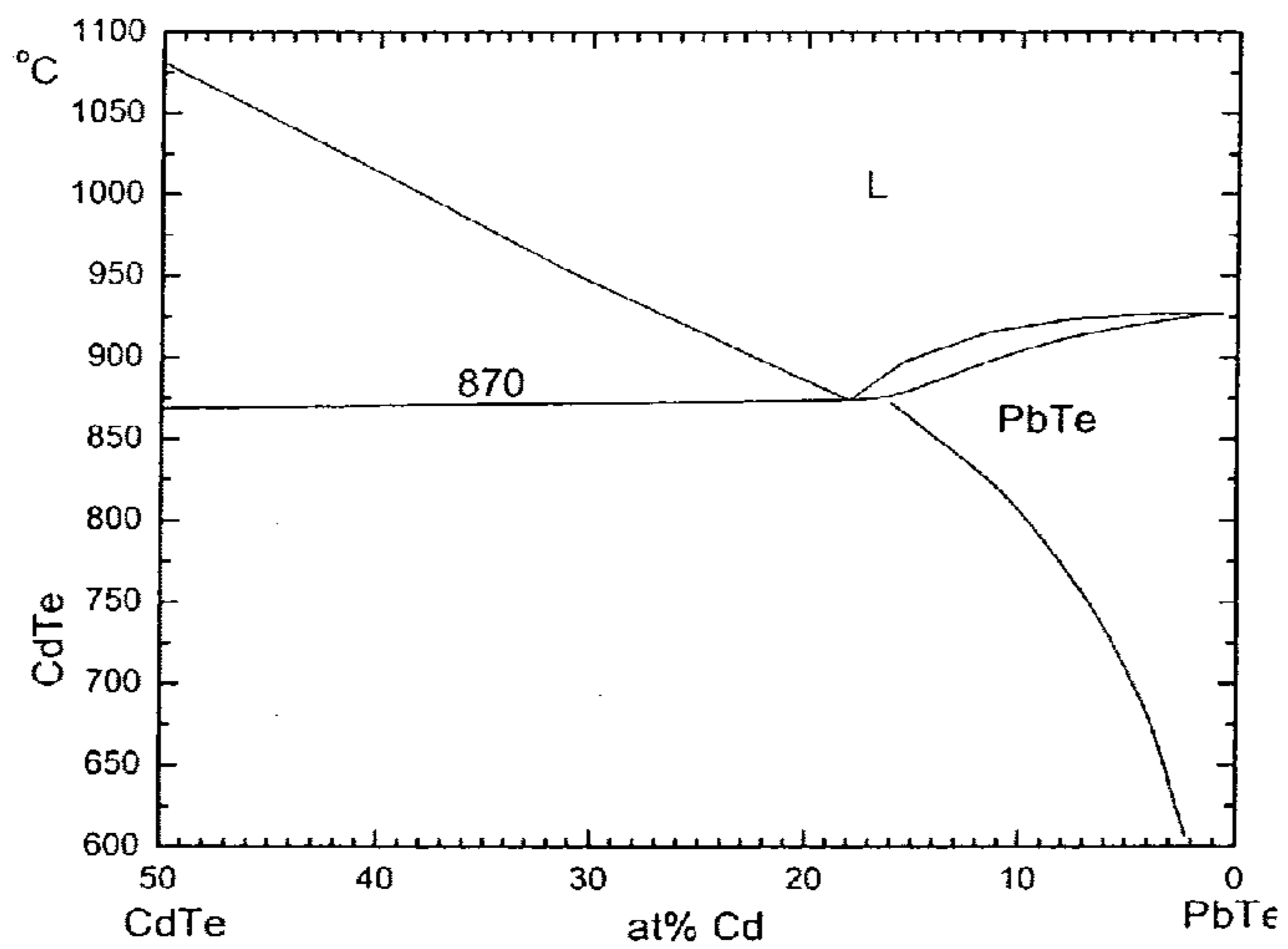


FIGURE 9D

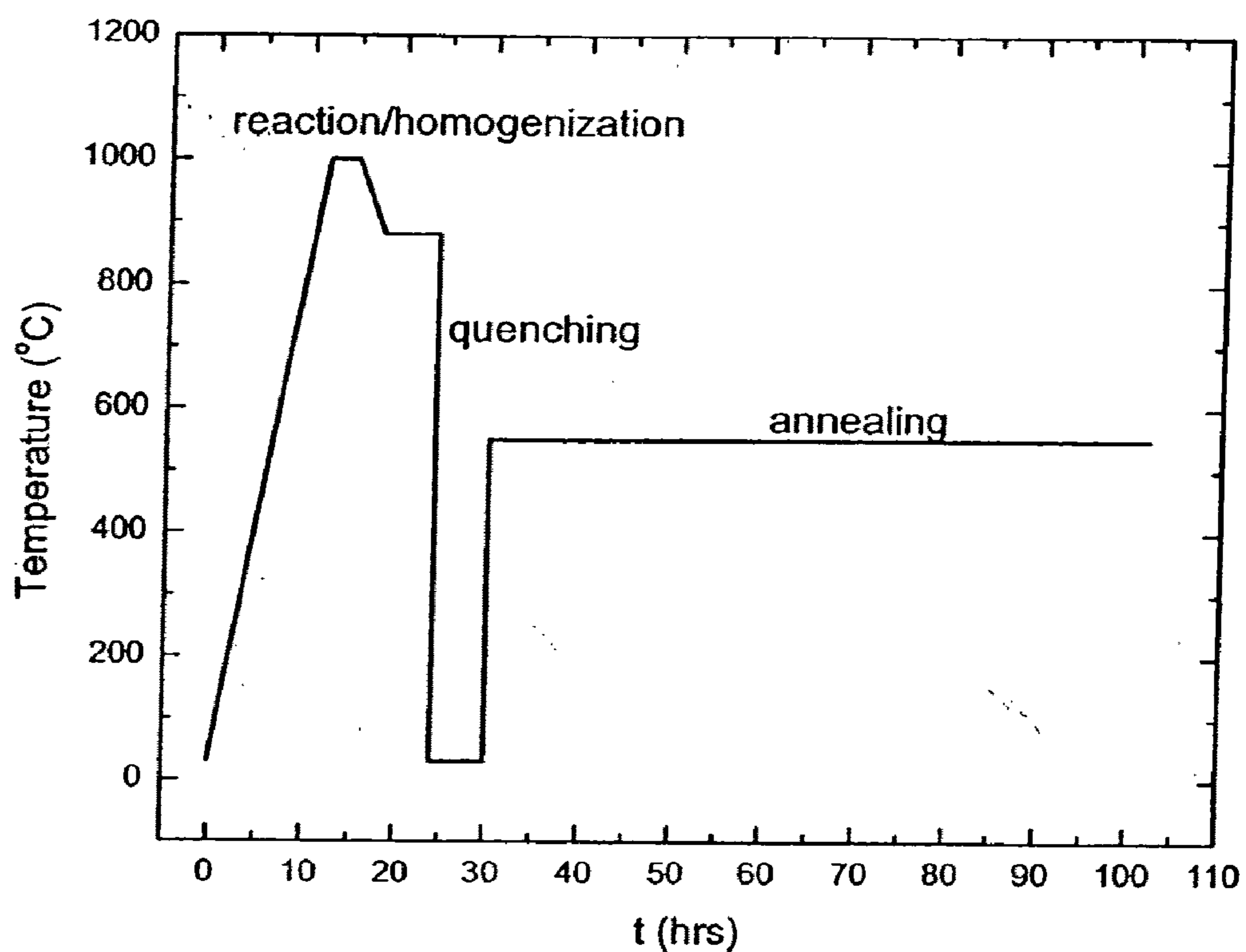


FIGURE 9E

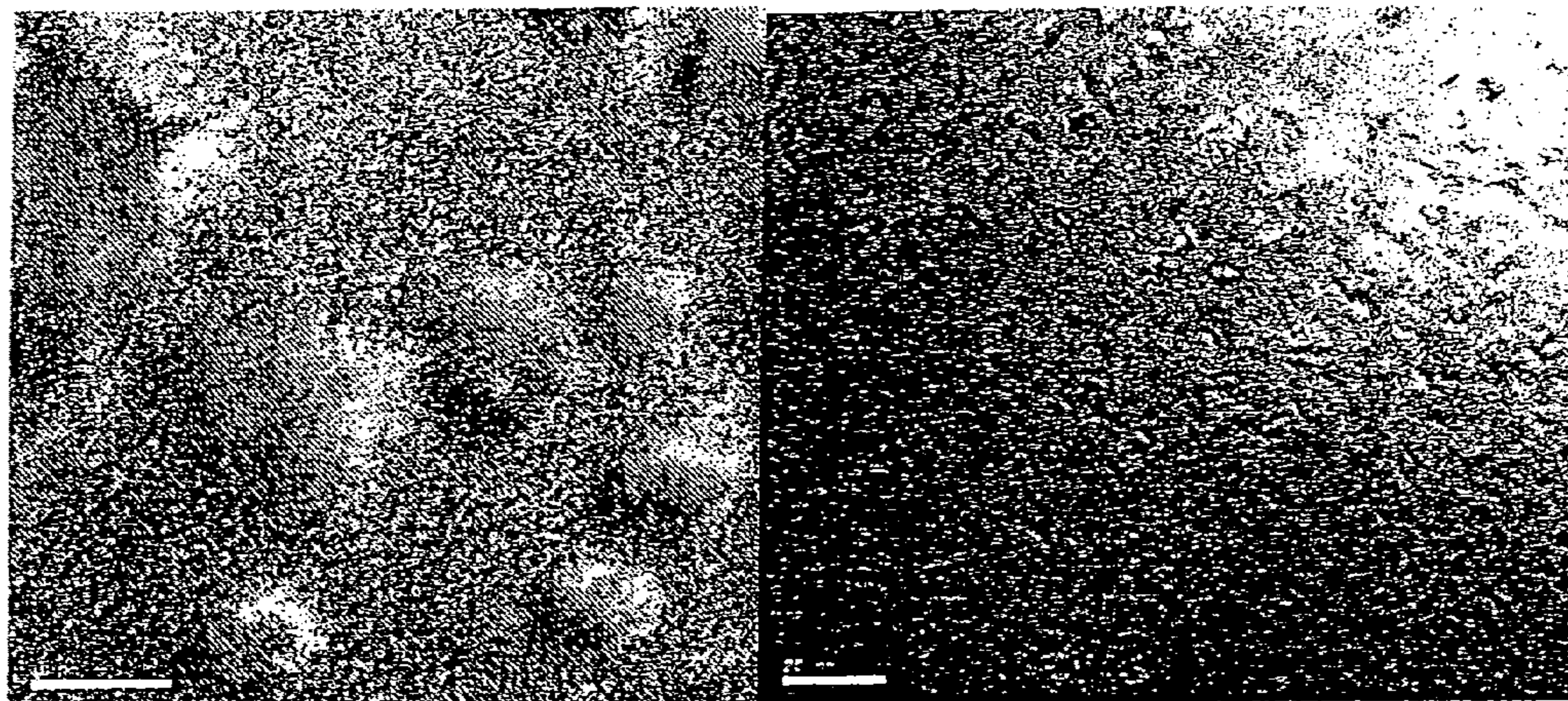


FIGURE 9F

FIGURE 9G

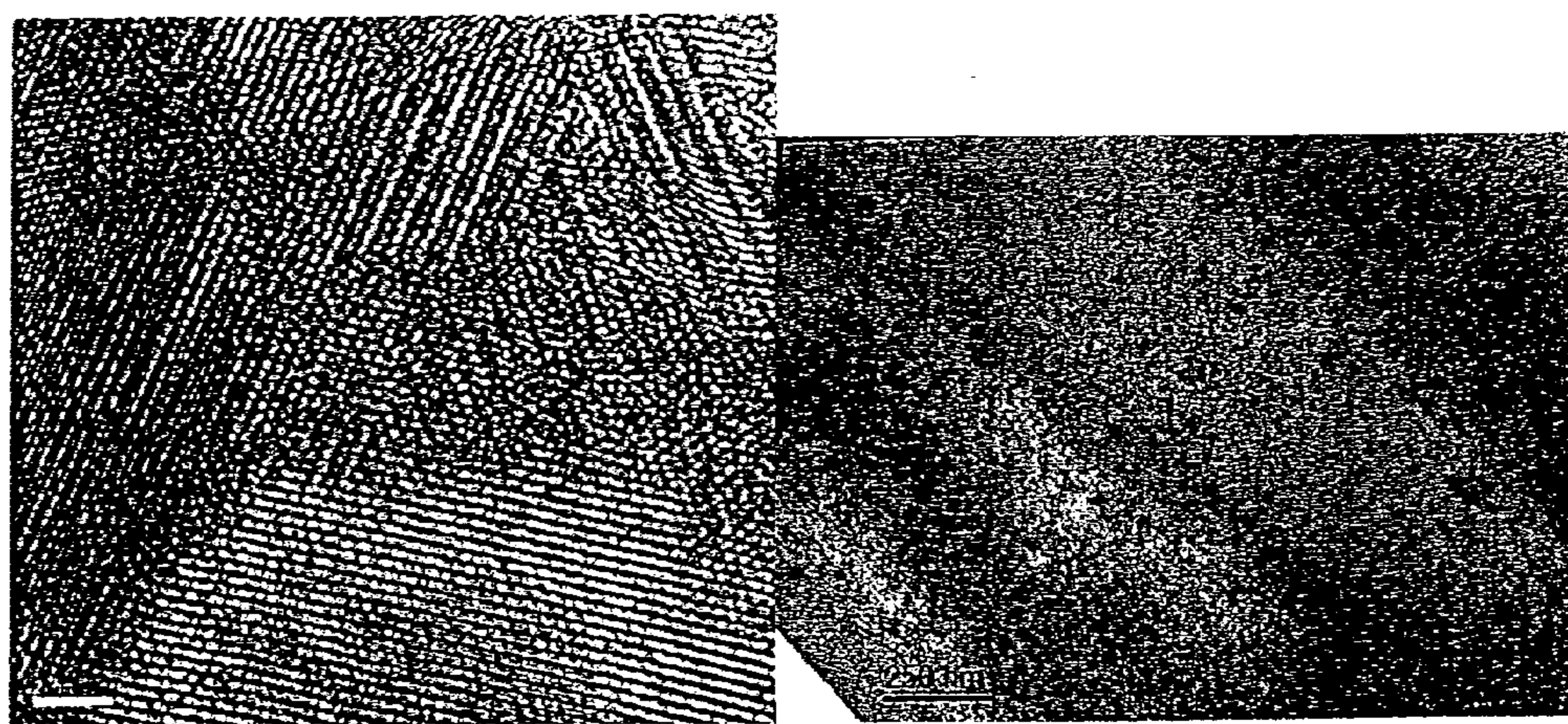


FIGURE 9H

FIGURE 9I

## THERMOELECTRIC COMPOSITIONS AND PROCESS

### CROSS-REFERENCE TO RELATED APPLICATIONS

**[0001]** This application is a divisional of U.S. patent application Ser. No. 11/445,662 filed Jun. 2, 2006 and incorporated in its entirety by reference herein, which claims the benefit of U.S. Provisional Patent Application No. 60/687,769 filed Jun. 6, 2005.

### BACKGROUND OF THE INVENTION

**[0002]** 1. Field of the Invention

**[0003]** The present invention relates to a process for producing novel bulk thermoelectric compositions with nanoscale inclusions which enhance the figure of merit (ZT). In particular, the present invention relates to thermoelectric compositions wherein the nanoscale inclusions are visible by conventional nanoscale imaging techniques such as transmission electron microscopy (TEM) imaging. They are useful for power generation and heat pumps.

**[0004]** 2. Description of the Related Art

**[0005]** The prior art in thermoelectric materials and devices is generally described in U.S. Pat. No. 5,448,109 to Cauchy, U.S. Pat. No. 6,312,617 to Kanatzidis et al., as well as published application 2004/0200519 A1 to Sterzel et al. and 2005/0076944 A1 to Kanatzidis et al. Each of these references is concerned with increasing the figure of merit (ZT) which is directly influenced by the product of electrical conductivity and the square of the thermopower divided by the thermal conductivity. Generally as the electrical conductivity of a thermoelectric material is increased, the thermal conductivity is increased. The efficiency of the thermoelectric device is less than theoretical and may not be sufficiently efficient for commercial purposes.

### SUMMARY OF THE INVENTION

**[0006]** It is therefore an object of the present invention to provide relatively efficient bulk thermoelectric materials. Further, it is an object of the present invention to provide a process for the preparation of these thermoelectric materials. Further, it is an object of the present invention to provide thermoelectric materials which are relatively economical to prepare compared to artificial deposited superlattice thin film thermoelectric materials. These and other objects will become increasingly apparent by reference to the following description and the drawings.

**[0007]** The present invention relates to a thermoelectric composition which comprises: a homogenous solid solution or compound of a first chalcogenide providing a matrix with nanoscale inclusions of a second phase which has a different composition wherein a figure of merit (ZT) of the composition is greater than that without the inclusions. Preferably the inclusion has been formed by spinodal decomposition as a result of annealing the composition at an appropriate temperature less than a melting point of the homogenous solid solution based upon a phase diagram. Preferably the inclusion has been formed by matrix encapsulation as a result of doping of a mol ten solution of the matrix. Preferably the inclusion has been formed by nucleation and growth of the inclusion by cooling a molten solution of the matrix.

**[0008]** The present invention also relates to a thermoelectric composition which comprises a homogenous solid solu-

tion or compound of a chalcogenide comprising a uniform precipitated dispersion of nano particles of at least two different metal chalcogenides wherein the chalcogen is selected from the group consisting of tellurium, sulfur and selenium. Preferably the composition has been formed by spinodal decomposition of the solid solution.

**[0009]** The present invention also relates to a thermoelectric composition which comprises a homogenous solid solution or compound of a chalcogenide with dispersed nano particles derived from a metal or a semiconductor which have been added to the chalcogenide.

**[0010]** The present invention also relates to a thermoelectric composition which comprises a homogenous solid solution or compound of a chalcogenide which has been annealed at a temperature which allows the formation of nano particles having a different composition than the solid solution or compound.

**[0011]** Further, the present invention relates to a composition wherein the inclusion has been formed by matrix encapsulation as a result of doping of a molten solution of the matrix.

**[0012]** Still further, the present invention relates to a composition wherein the inclusion has been formed by nucleation and growth of the inclusion by cooling a molten solution of the matrix.

**[0013]** The present invention further relates to a process for preparing a thermoelectric composition which comprises:

**[0014]** (a) forming a liquid solution or compound of a first chalcogenide and a second phase which has a different composition;

**[0015]** (b) cooling the solution rapidly so that a solid solution of the first chalcogenide as a matrix and the second phase as a nanoscale inclusion is formed, so that the figure of merit is greater than without the inclusions. Preferably the inclusion is formed by spinodal decomposition as a result of annealing the composition at an appropriate temperature less than a melting point of the homogenous solid solution based upon a phase diagram. Preferably the inclusion is formed by matrix encapsulation as a result of cooling a molten solution of the matrix. Preferably the inclusion is formed by nucleation and growth of the inclusion in a supersaturated solid solution of the matrix. Preferably the chalcogenides are of a chalcogen selected from the group consisting of tellurium, sulfur and selenium. Preferably the inclusions are between about 1 and 200 nanometers.

**[0016]** The substance and advantages of the present invention will become increasingly apparent by reference to the following drawings and the description.

### BRIEF DESCRIPTION OF THE DRAWINGS

**[0017]** FIG. 1 is a graph showing the lowest thermal conductivity exhibited by the PbTe—PbS 16% nanocomposite.

**[0018]** FIG. 2A is a theoretical phase diagram for A and B.

**[0019]** FIG. 2B is a diagram showing the spatial difference in the composition of the phases.

**[0020]** FIG. 3A shows a PbTe—PbS phase diagram. FIG. 3B is a PbTe—PbS x % nano-composite reaction and post-annealing profile taking advantage of spinodal decomposition. FIGS. 3C and 3D are high resolution TEM images of a PbTe—PbS 16% spinodally decomposed system.

**[0021]** FIG. 4A is a schematic of the matrix encapsulation. FIG. 4B is a graph of a PbTe—Sb heating profile. FIG. 4C is a PbTe—Sb (2%) Bright Field Image. FIGS. 4D and 4E are corresponding Bright and Dark Field TEM images of PbTe—



InSb (2%). FIGS. 4F to 4K are transmission electron micrographs showing dispersed nanoparticles of Sb within a crystalline matrix of PbTe. Similar size, shape, and volume fraction are observed for (A) PbTe—Sb (2%) (B) PbTe—Sb (4%) (C) PbTe—Sb (8%) and (D) PbTe—Sb (16%). Because the 8 and 16% samples contain distinct Sb regions the images shown in FIGS. 4C and 4D are from the PbTe rich region. FIG. 4E is a high resolution transmission electron micrograph showing several nanoprecipitates of Sb coherently embedded within the matrix of PbTe. Embedded particles help to maintain high electron mobility while serving as a site for phonon scattering to reduce the thermal conductivity. FIG. 4F is a high resolution micrograph of the PbTe—Bi (4%) system also showing embedded particles in the PbTe matrix. FIG. 4L is a graph showing thermal conductivity as a function of temperature.

[0022] FIGS. 5A and 5B are scanning electron micrographs of PbTe+Pb (2%)+Sb (3%). Large regions or ribbons, several hundred microns in length, composed of a Pb—Sb eutectic appear throughout the sample. Similar microstructure is observed for other samples with similar composition.

[0023] FIGS. 6A and 6B show powder x-ray diffraction clearly indicating additional phases of Pb and Sb as revealed by the magnified inset between 25 and 40 degrees. The peak at ~29 deg. corresponds to elemental Sb while the peaks at 31 and 36 deg. can be indexed according to elemental Pb.

[0024] FIGS. 7A and 7B show (7A) low magnification transmission electron micrographs showing dispersed particles of Pb and Sb within the PbTe matrix. FIG. 7B shows high magnification TEM micrographs showing the particles appear coherently embedded in the matrix.

[0025] FIG. 8 is a graph showing lattice thermal conductivity as a function of Pb/Sb ratio at 350K and 600K. A strong linear dependence of the lattice thermal conductivity is observed as the ratio is varied.

[0026] FIG. 9A is a schematic diagram of supersaturated solid solution produced through quenching. FIG. 9B is a schematic diagram of a post annealing within the two phase region of the phase diagram which initiates the coalescence of the second phase into ordered nano-precipitates. FIG. 9C is a schematic diagram of a coherent nano-particle which has been formed. FIG. 9D is a PbTe—CdTe phase diagram. FIG. 9E is a graph of PbTe—CdTe x % reaction and post annealing profile for  $2 \leq x \leq 9$ . FIGS. 9F and 9G are TEM images of PbS—PbTe6%, and FIGS. 9H and 9I are TEM images of PbTe—CdTe9%.

#### DETAILED DESCRIPTION OF THE PREFERRED EMBODIMENT

[0027] The bulk materials containing nanometer-sized inclusions provide enhanced thermoelectric properties. The thermoelectric figure of merit is improved by reducing the thermal conductivity while maintaining or increasing the electrical conductivity and the Seebeck coefficient. Coherent nanometer sized inclusions in a matrix can serve as sites for scattering of phonons that subsequently lower the thermal conductivity. General methods for preparation of these materials have been developed.

[0028] The thermoelectric heat to electricity converters will play a key role in future energy conservation, management, and utilization. Thermoelectric coolers also play an important role in electronics and other industries. More efficient thermoelectric materials need to be identified in order to extend their use in power generation and cooling applications.

[0029] As previously noted, the measure used to determine the quality of a thermoelectric material is the dimensionless figure of merit  $ZT$ , where  $ZT = (\sigma S^2 / \kappa) T$ , where  $\sigma$  is the electrical conductivity,  $S$  the Seebeck coefficient or the absolute thermopower,  $T$  is the temperature and  $\kappa$  is the thermal conductivity. The quantity  $\sigma S^2$  is called the power factor. The goal is then to simultaneously improve the thermopower, electrical conductivity (i.e. the power factor), and reduce the thermal conductivity thereby raising  $ZT$ . The aforementioned properties are intimately related.

[0030] PbTe and Si/Ge alloys are the current thermoelectric materials used for power generation. These compounds once doped possess a maximum  $ZT$  of approximately 0.8 at 600 K and 1200 K respectively. By lowering the thermal conductivity of these materials the  $ZT$  can be improved without sacrificing the properties already known. Currently  $\text{Bi}_2\text{Te}_3$  and its alloys with  $\text{Bi}_2\text{Se}_3$  and  $\text{Sb}_2\text{Te}_3$ , along with alloys of Bi and Sb, are considered the state of the art in terms of thermoelectric cooling materials. These materials have been modified in many ways chemically in order to optimize their performance, however significant improvements can be made to enhance the properties of the currently used thermoelectric materials.

[0031] Increasing the efficiency of a thermoelectric material usually involves raising the scattering rate of phonons while at the same time maintaining high carrier mobility. In this respect, it has been demonstrated that thin-film superlattice materials have enhanced  $ZT$  that can be explained by the decrease in the thermal conductivity. A superlattice structure creates de facto a complex arrangement of structural interfaces which in effect raises the thermal resistance of propagating phonons. On the other hand, lattice-matching and coherence of the interfaces ensures undisturbed electron flow thus maintaining a high mobility. This decoupling of electrical and lattice thermal conductivity is necessary to reduce the total thermal conductivity without sacrificing the electrical conductivity.

[0032] The drawbacks of superlattice thin films are that they are expensive to prepare, difficult to grow, and will not easily support a large temperature difference across the material. It is thus desirable to incorporate inclusions on the nanometer length scale into a bulk material that is low cost, easy to manufacture, and can support a temperature gradient easily.

[0033] In the present invention, three methods have been employed in the production of the desired nanocomposite material for thermoelectric material fabrication. Each of these methods are discussed in detail in the following sections along with an example, Transmission Electron Microscope (TEM) images, and a table of materials systems that can be produced from each general method. The first, spinodal decomposition, has been used to create a material with compositional fluctuations on the nanometer length scale. The other two methods, matrix encapsulation and nucleation and growth, have shown the ability to produce inclusions of various materials inside a host matrix.

[0034] Phonon mean free paths,  $\iota_{ph}$ , in semiconducting crystals are in the range  $1 \leq \iota_{ph} \leq 100$  nm with a tendency to decrease with increasing temperatures. Realization of nanocomposite thermoelectric materials offer a way of introducing nano-meter sized scatterers that can greatly suppress the lattice thermal conductivity through phonon scattering. The existence of a wide particle size distribution offers the possibility of scattering a wider range of the phononic spectrum.

**[0035]** Experimental confirmation of the above at room temperature and below comes from the PbTe—PbS 16% at system as the plot of the lattice thermal conductivity shows in FIG. 1, a >40% reduction of the lattice thermal conductivity is observed in the case of the nano-precipitate specimen with respect to the perfect mixture of the same composition at room temperature.

**[0036]** It has been suggested that band gap or electron energy states engineering offer an alternative route to further enhancing the power factor of thermoelectric materials. Essentially the idea consists in the mixing of parabolic bands (bulk semiconductors) with reduced dimensionality structures (e.g. nano-dots exhibit a comb-like density of states) to produce a ripple effect on the resulting density of states of the composite.

**[0037]** Experimental confirmation of enhanced power factors come from the following systems shown in Table 1:

TABLE 1

Sample composition	Power factor ( $\mu\text{W}/\text{cmK}^2$ )	Temperature (K)
PbTe—PbS 16%: PbI <sub>2</sub> 0.05%	28	400
PbTe—CdTe 5%: PbI <sub>2</sub> 0.05%	30	300
PbTe—CdTe 9%	26	300
PbTe—Sb 4%	20	300
PbTe—InSb 2%	21	300
PbTe—Pb (0.5%)—Sb (2%)	28	300
PbTe—Pb (2%)—Sb (3%)	19	300

#### Method 1: Spinodal Decomposition

**[0038]** Spinodal decomposition refers to the way a stable single-phase mixture of two phases can be made unstable. Thermodynamically, the necessary condition for the stability or metastability of a heterogeneous phase is that the chemical potential of a component must increase with increasing density of that component. For two components this reduces to

$$\left. \frac{\partial^2 G}{\partial^2 X} \right|_{T,P} > 0,$$

where X is the concentration. If this condition is not met, the mixture is unstable with respect to continuous compositional variations and the limit of this metastability is called the spinodal defined as

$$\frac{\partial^2 G}{\partial^2 X} = 0,$$

where X is the concentration. Spinodal fluctuations do not involve any crystalline transformation, since both components of the mixed phase system are sharing the same lattice, but involves a spatial modulation of the local composition at the nanoscale. This spatial modulation was exploited to create coherently embedded nano-particles of a phase into a thermoelectric matrix and thus create nanostructured thermoelectric materials on a large reaction scale.

**[0039]** Consider a phase diagram with a miscibility gap, i.e. an area within the coexistence curve of an isobaric or an

isothermal phase diagram where there are at least two phases coexisting (see FIG. 2A). If a mixture of phases A and B and of composition  $X_0$  is solution treated at a high temperature  $T_1$  and then quenched at to a lower temperature  $T_2$  the composition instantly will be the same everywhere (ideal solid solution) and hence the system's free energy will be  $G_0$  on the  $G(X)$  curve. However, infinitesimal compositional fluctuations cause the system to locally produce A-rich and B-rich regions. The system now has become unstable since the total free energy has decreased. In time, the system decomposes until the equilibrium compositions  $X_1$  and  $X_2$  are reached throughout the system (compare FIG. 2A and FIG. 2B).

**[0040]** There are two major advantages in the application of the spinodal decomposition process in order to produce thermoelectric nanocomposites; (a) thermodynamic principles define the spatial modulation wavelength  $\lambda$  to be in the range nm which is a very desirable phonon-scattering length scale and (b) the nano-structure is thermodynamically stable. Therefore, spinodally decomposed thermoelectric materials are naturally produced bulk nanocomposites which can be perpetually stable when used within a specified temperature region defined by the phase diagram.

**[0041]** The aforementioned procedure was applied extensively in the PbTe—PbS system where PbTe serves as the matrix.

#### Example

##### PbTe—PbS x % Preparation Example

**[0042]** Spinodal decomposition in the two components system PbTe—PbS x % occurs for  $\sim 4 \leq x \leq 96\%$  for temperatures roughly below  $700^\circ \text{C}$ . (see accompanying phase diagram FIG. 3A). The high purity starting materials are mixed in aqua regia cleaned fused silica tubes and fired according to the reaction profile shown in FIG. 3B.

**[0043]** The TEM images of spinodally decomposed system PbTe—PbS 16% are shown in FIGS. 3C, 3D.

**[0044]** The following Table 2 show systems that can be produced to exist in a nanostructured state via the Spinodal Decomposition mechanism. The listing is a set of materials composed of component A and B in a  $A_{1-x}B_x$  stoichiometry ( $0 < x < 1$ ).

TABLE 2

Spinodal Decomposition A-B
PbTe—PbS
AgSbTe <sub>2</sub> —SnTe
PbS—PbTe
SnTe/SnSe
SnTe/PbS
SnTe/PbSe
SnTe/SnSe
SnSe/PbS
SnSe/PbSe
SnSe/PbTe
AgSbSe <sub>2</sub> —SnTe
AgSbTe <sub>2</sub> —SnSe
AgSbSe <sub>2</sub> —PbTe
AgSbS <sub>2</sub> —PbTe
SnTe—REPn (RE = rare earth element, Pn = P, As, Sb, Bi)
PbTe—REPn (RE = rare earth element, Pn = P, As, Sb, Bi)
PbSe—REPn (RE = rare earth element, Pn = P, As, Sb, Bi)

TABLE 2-continued

Spinodal Decomposition A-B
SnSe—RE <sub>n</sub> Pn (RE = rare earth element, Pn = P, As, Sb, Bi)

## Method 2: Matrix Encapsulation

**[0045]** These systems, as described by a phase diagram, should have a solid solution in the composition range of approximately 0.1-15% of the minor phase. However, it has been observed that, when quenched from a melt, these systems exhibit inclusions on the nanometer scale of the minor phase material. This phenomenon can be extended to other systems of thermoelectric interest where the matrix is a good thermoelectric and the minor phase is a material that is non-reactive, has a lower melting point, and is soluble with the matrix in the liquid state. The minor phase may also be a mixture of two or more of these non-reactive materials which may or may not form a compound themselves. These materials must be quenched quickly through the melting point of the matrix in order to freeze the minor phase. After quenching the samples must be post annealed to improve crystallinity and thermoelectric properties.

## Example

**[0046]** This method has been applied to PbTe—Sb, PbTe—Bi, PbTe—InSb and PbTe—Pb—Sb showing promise in each of the cases.

## PbTe—Sb 4% Preparation Example

**[0047]** Lead telluride and antimony were combined in the appropriate molar ratio and sealed in an evacuated fused silica tube and heated according to the profile shown in FIG. 4B. The bright field and dark field images are shown in FIGS. 4C to 4E. The TEM images of encapsulated nanoparticles are shown in FIGS. 4F to 4K. FIG. 4L shows the lattice thermal conductivity.

**[0048]** Table 3 shows systems for Matrix Encapsulation listing the matrix and precipitate.

## Matrix Encapsulation Using Two or More Types of Nanophase Particles:

**[0049]** It is possible to produce samples via the matrix encapsulation method which have multiple nanoscale inclusions (two or more from those listed in Table 3).

**[0050]** These inclusions may be used to combine the favorable properties of each to produce a superior thermoelectric material. The additional phases must also be soluble with the matrix in the liquid state, may or may not be reactive with the matrix, and may or may not form a compound between each other. This method has been applied to PbTe with inclusions of both Sb and Pb with interesting behavior in terms of both the reduction of the thermal conductivity, and modification of the behavior of the electrical transport as well. The ratio of Pb to Sb can modify the conductivity such that a higher electrical conductivity may be maintained through the desired temperature range. The mass fluctuations associated with the addi-

tional phase reduce the thermal conductivity as seen in the previously discussed examples.

## PbTe—Pb—Sb Preparation Example

**[0051]** Pb, Sb, and Te were sealed in an evacuated fused silica tube and heated to the molten state. The tube was then removed from the high temperature furnace for rapid cooling of the melt. This procedure is similar to those discussed above, however multiple nanoprecipitate inclusion phases are used rather than a single component inclusion. Many different possible inclusion combinations are possible and one example, the PbTe—Pb—Sb case, is given below.

**[0052]** SEM micrographs (FIGS. 5A and 5B), Powder X-ray diffraction (FIGS. 6A and 6B), TEM micrographs (FIGS. 7A and 7B), and experimental power factors and thermal conductivity values (FIG. 8). These systems represent an interesting set of materials in which the transport properties can be tuned by several variables such as total concentration, ratio of various inclusion phases, and the properties of the inclusions themselves. Optimization is still underway and ZT values of over 1 have been obtained in the as-prepared systems.

TABLE 3

Matrix Encapsulation A(matrix)-B(precipitate)
Pb(Te,Se,S)—Sb,Bi,As
Pb(Te,Se,S)—(InSb,GaSb)
Pb(Te,Se,S)—Yb
Pb(Te,Se,S)—(InAs,GaAs)
Pb(Te,Se,S)—Eu
Pb(Te,Se,S)—In
Pb(Te,Se,S)—Ga
Pb(Te,Se,S)—Al
Pb(Te,Se,S)—Zn
Pb(Te,Se,S)—Cd
Pb(Te,Se,S)—Sn
Pb(Te,Se,S)—TlInQ2*
Pb(Te,Se,S)—Zn <sub>x</sub> Sb <sub>y</sub>
Pb(Te,Se,S)—AgYb
Pb(Te,Se,S)—CdPd
Pb(Te,Ae,S)—RE <sub>2</sub> Pb <sub>3</sub>
(RE = rare earth element, Y)
Pb(Te,Se,S)—M
(M = Ge, Sn, Pb)
Pb(Te,Se,S)—Ag <sub>4</sub> Eu
Pb(Te,Se,S)—AgEu
Pb(Te,Se,S)—AgCe
Pb(Te,Se,S)—Mg <sub>2</sub> Cu
Pb(Te,Se,S)—Cu <sub>2</sub> La
Pb(Te,Se,S)—Cu <sub>6</sub> Eu
Pb(Te,Se,S)—Eu <sub>3</sub> Pd <sub>2</sub>
Pb(Te,Se,S)—Mg <sub>2</sub> Eu
Pb(Te,Se,S)—PdTe <sub>2</sub>
Pb(Te,Se,S)—Mg <sub>2</sub> Sn
Pb(Te,Se,S)—MgSm
Pb(Te,Se,S)—MgPr
Pb(Te,Se,S)—Mg <sub>2</sub> Pb
Pb(Te,Se,S)—Ca <sub>84</sub> Ni <sub>16</sub>
Pb(Te,Se,S)—RE <sub>2</sub> Pb
(RE = rare earth element)
Pb(Te,Se,S)—Mg <sub>2</sub> Pb
Pb(Te,Se,S)—RE <sub>2</sub> Pb
(RE = rare earth element)

\*Q = S,Se,Te

## Method 3: Nucleation and Growth Mechanism:

**[0053]** The method of nucleation and growth of nanoparticles within the matrix of a thermoelectric material consists

of three distinct thermal treatments that depend crucially on the phase diagram of the composite:

**[0054]** a) The starting materials (mixed in appropriate stoichiometry) are heated from the two-phase region to the single-phase region of the phase diagram to dissolve all precipitates. The mixture is held there for several hours to ensure complete homogeneity;

**[0055]** b) The melt or solid solution is quenched to room temperature using different methods: air quenching, water quenching, ice water quenching. This freezes the high temperature homogenous phase into a supersaturated solid solution; and

**[0056]** c) Depending on the kinetics of the specific system the specimen is post annealed at an elevated temperature within the two-phase region of the phase diagram and is held there for several hours to allow the nanoprecipitates to form and grow. Annealing time and temperature is proportional to the size growth of the precipitates. Therefore, the size of the nanoprecipitates can be controlled through careful selection of annealing time and temperature.

**[0057]** The following schematic shows in FIGS. 9A, 9B and 9C roughly how the nano-precipitation of the second phase is taking place.

**[0058]** As a general rule this kind of nanostructured thermoelectric materials should meet two conditions: (1) The two phases should contain elements that enter a solid solution phase at a specific temperature and separate into a mixture at another lower temperature. (2) The phase that precipitates out must create a coherent or at best semi-coherent precipitate. Coherency is important since it ensures bonding with the lattice of the matrix and hence the precipitate does not act as a strong scatterer to the electrons.

**[0059]** The above procedure has been extensively applied to the PbTe—CdTe system with excellent results.

#### Example

##### PbTe—CdTe x % Preparation Example

**[0060]** Stoichiometric quantities of Pb, Te and Cd are weighed targeting x % values in the range  $2 \leq x \leq 9$ . The starting materials are placed in graphite crucibles, which are subsequently sealed under high vacuum in fused silica tubes and fired according to the reaction profile shown below (FIG. 9E). The reaction profile is decided based on the phase diagram of the PbTe—CdTe system (FIG. 9D). FIGS. 9F and 9G show the TEM images for precipitation and growth of PbS—PbTe 6%. FIGS. 9H and 9I show the system PbTe—CdTe 9%.

**[0061]** The following Table 4 shows systems for nucleation and growth listing the matrix and precipitate.

TABLE 4

Nucleation and Growth A(matrix)-B(precipitate)
PbSe—Sb <sub>2</sub> Se <sub>3</sub>
PbSe—SnSe <sub>2</sub>
PbSe—Zn
PbTe—Hg <sub>1-x</sub> Cd <sub>x</sub> Te (0 < x < 1)
PbTe—ZnTe
PbTe—Sb <sub>2</sub> Se <sub>3</sub>
PbTe—Zn
PbTe—In <sub>2</sub> Se <sub>3</sub>
PbTe—In <sub>2</sub> Te <sub>3</sub>
PbTe—Ga <sub>2</sub> Te <sub>3</sub>
PbTe—AgInTe <sub>2</sub>

TABLE 4-continued

Nucleation and Growth A(matrix)-B(precipitate)
PbTe—CuInTe <sub>2</sub>
PbTe—CuInSe <sub>2</sub>
PbTe—CuInTe <sub>2</sub>
PbSe—Hg <sub>1-x</sub> Cd <sub>x</sub> Q (0 < x < 1, Q = S, Se, Te)
PbSe—ZnTe
PbSe—In <sub>2</sub> Se <sub>3</sub>
PbSe—In <sub>2</sub> Te <sub>3</sub>
PbSe—Ga <sub>2</sub> Te <sub>3</sub>
PbSe—AgInSe <sub>2</sub>
PbSe—CuInTe <sub>2</sub>
PbSe—CuInSe <sub>2</sub>
PbSe—CuInTe <sub>2</sub>

**[0062]** It is intended that the foregoing description be only illustrative of the present invention and that the present invention be limited only by the hereinafter appended claims.

What is claimed is:

1. A thermoelectric composition comprising: a matrix comprising a first chalcogenide; and nanoscale inclusions in the matrix, the nanoscale inclusions being coherent or semi-coherent with the matrix, the nanoscale inclusions having a different composition than the first chalcogenide, so that the nanoscale inclusions decrease the thermal conductivity of the composition by scattering phonons in the composition while substantially maintaining or increasing electrical conductivity and Seebeck coefficient of the composition.
2. The thermoelectric composition of claim 1, wherein the nanoscale inclusions are coherent with the matrix.
3. The thermoelectric composition of claim 1, wherein the nanoscale inclusions have a first melting point, the matrix has a second melting point, and the first melting point is lower than the second melting point.
4. The thermoelectric composition of claim 1, wherein the nanoscale inclusions have a first melting point, the matrix has a second melting point, and the second melting point is lower than the first melting point.
5. The thermoelectric composition of claim 1, wherein the nanoscale inclusions have a first melting point, the matrix has a second melting point, and the first melting point is different than the second melting point.
6. The thermoelectric composition of claim 1, wherein at least a portion of the nanoscale inclusions are a uniform dispersion of nanoparticles.
7. The thermoelectric composition of claim 1, wherein about 0.1 to 15% of the composition comprises the nanoscale inclusions.
8. The thermoelectric composition of claim 1, wherein at least a portion of the nanoscale inclusions comprise a material that is nonreactive, has a lower melting point, and is soluble with the matrix in a liquid state.
9. The thermoelectric composition of claim 1, wherein the first chalcogenide comprises a chalcogen selected from the group consisting of tellurium, sulfur and selenium.
10. The thermoelectric composition of claim 1, wherein at least a portion of the nanoscale inclusions have a size between about 1 and 200 nanometers.
11. The thermoelectric composition of claim 1, wherein the nanoscale inclusions comprise multiple types of inclusions, each type having a different chemistry.

**12.** The thermoelectric composition of claim 1, wherein the composition has lattice thermal conductivity which is more than 40% reduced as compared to lattice thermal conductivity of the matrix.

**13.** The thermoelectric composition of claim 1, wherein the matrix comprises PbTe.

**14.** The thermoelectric composition of claim 13, wherein the nanoscale inclusions comprise PbS.

**15.** The thermoelectric composition of claim 13, wherein the nanoscale inclusions comprise at least one element selected from the group consisting of antimony, bismuth, and arsenic.

**16.** The thermoelectric composition of claim 13, wherein the nanoscale inclusions comprise lead and antimony.

**17.** The thermoelectric composition of claim 13, wherein the nanoscale inclusions comprise  $\text{Cd}_{1-x}\text{Hg}_x\text{Te}$  and  $0 < x < 1$ .

**18.** The thermoelectric composition of claim 1, wherein the matrix comprises PbS and the nanoscale inclusions comprise PbTe.

**19.** The thermoelectric composition of claim 1, wherein the nanoscale inclusions comprise a metal.

**20.** The thermoelectric composition of claim 1, wherein the nanoscale inclusions comprise a semiconductor.

**21.** The thermoelectric composition of claim 1, wherein the nanoscale inclusions comprise a second chalcogenide different from the first chalcogenide, the second chalcogenide comprising a chalcogen selected from the group consisting of tellurium, sulfur and selenium.

**22.** The thermoelectric composition of claim 1, wherein the matrix comprises PbQ, and the Q component comprises at least one element selected from the group consisting of: tellurium, selenium, and sulfur.

**23.** The thermoelectric composition of claim 1, wherein the matrix comprises SnQ, and the Q component comprises at least one element selected from the group consisting of: tellurium and selenium.

**24.** The thermoelectric composition of claim 1, wherein the nanoscale inclusions do not act as a strong scatterer to electrons.

**25.** The thermoelectric composition of claim 1, wherein at least a portion of the inclusions in the matrix are thermally stable to a temperature higher than 650 K.

**26.** The thermoelectric composition of claim 1, wherein the composition comprises a bulk composition.

**27.** A thermoelectric composition comprising:  
a matrix comprising a first chalcogenide; and

nanoscale inclusions in the matrix, the nanoscale inclusions have a first melting point, the matrix has a second melting point, the first melting point is lower than the second melting point, the nanoscale inclusions having a different composition than the first chalcogenide, so that the nanoscale inclusions decrease the thermal conductivity of the composition by scattering phonons in the composition while substantially maintaining or increasing electrical conductivity and Seebeck coefficient of the composition.

**28.** A thermoelectric composition comprising:  
a matrix comprising a first chalcogenide; and

nanoscale inclusions in the matrix, the nanoscale inclusions comprise a second chalcogenide different from the first chalcogenide, the second chalcogenide comprising a chalcogen selected from the group consisting of tellurium, sulfur and selenium, so that the nano scale inclusions decrease the thermal conductivity of the composition by scattering phonons in the composition while substantially maintaining or increasing electrical conductivity and Seebeck coefficient of the composition.

\* \* \* \* \*